Published in final edited form as:
*Matrix Biol*. 2014 June ; 36: 51–63. doi:10.1016/j.matbio.2014.04.004.

# Changes in type II procollagen isoform expression during chondrogenesis by disruption of an alternative 5' splice site within *Col2a1* exon 2

**Thomas M. Hering**[1,2], **Louisa Wirthlin**[2], **Soumya Ravindran**[2], and **Audrey McAlinden**[2,3,*]

[1]Spinal Cord and Brain Injury Research Center, Department of Anatomy & Neurobiology, University of Kentucky, Lexington, KY 40536

[2]Department of Orthopaedic Surgery, Washington University School of Medicine, St Louis, MO 63110

[3]Department Cell Biology & Physiology, Washington University School of Medicine, St Louis, MO 63110

## Abstract

This study describes a new mechanism controlling the production of alternatively-spliced isoforms of type II procollagen (*Col2a1*) *in vivo*. During chondrogenesis, precursor chondrocytes predominantly produce isoforms containing alternatively-spliced exon 2 (type IIA and IID) while *Col2a1* mRNA devoid of exon 2 (type IIB) is the major isoform produced by differentiated chondrocytes. We previously identified an additional *Col2a1* isoform containing a truncated exon 2 and premature termination codons in exon 6 (type IIC). This transcript is produced by utilization of another 5' splice site present in exon 2. To determine the role of this IIC splicing event *in vivo*, we generated transgenic mice containing silent knock-in mutations at the IIC 5' splice site (*Col2a1-mIIC*), thereby inhibiting production of IIC transcripts. Heterozygous and homozygous knock-in mice were viable and display no overt skeletal phenotype to date. However, RNA expression profiles revealed that chondrocytes in cartilage from an age range of *Col2a1-mIIC* mice produced higher levels of IIA and IID mRNAs and decreased levels of IIB mRNAs throughout pre-natal and post-natal development, when compared to chondrocytes from littermate control mice. Immunofluorescence analyses showed a clear increase in expression of embryonic type II collagen protein isoforms (i.e. containing the exon 2-encoded cysteine-rich (CR) protein domain) in cartilage extracellular matrix (ECM). Interestingly, at P14, P28 and P56, expression of embryonic Col2a1 isoforms in *Col2a1-mIIC* mice persisted in the pericellular domain of the ECM in articular and growth plate cartilage. We also show that persistent expression of the exon 2-encoded CR domain in the ECM of post-natal cartilage tissue may be due, in part, to the embryonic form of type XI collagen (the α3 chain of which is also encoded by the *Col2a1* gene). In conclusion, expression of the *Col2a1* IIC splice form may have a regulatory function in controlling alternative splicing of exon 2 to generate defined proportions of IIA, IID and IIB procollagen isoforms during cartilage development. Future studies will involve ultrastructural and

[*]Audrey McAlinden, Ph.D. Department of Orthopaedic Surgery, Department of Cell Biology and Physiology, Musculoskeletal Research Center, Washington University School of Medicine, 660 South Euclid Avenue, St Louis, MO 63110, Tel: 314-454-8860, Fax: 314-454-5900, mcalindena@wudosis.wustl.edu.

biomechanical analysis of the collagen ECM to determine the effects of persistent mis-expression of embryonic collagen isoforms in mature cartilage tissue.

**Keywords**

type II procollagen (*Col2a1*); precursor (pre)-mRNA; alternative splicing; chondrocyte; extracellular matrix; knock-in transgenic mouse

## 1. Introduction

The type II procollagen gene (*Col2a1*) encodes α1(II) chains that form homotrimeric procollagens consisting of a triple-helical fibrillar domain flanked by a 5' amino ($NH_2$) propeptide and 3' carboxy (COOH) propeptide. The $NH_2$ and COOH propeptides are removed by specific proteases resulting in processed triple-helical collagen molecules that form cross-linked fibrils in the extracellular matrix (ECM) of cartilage tissue (Canty and Kadler, 2005; Eyre, 2002; Eyre et al., 2006; Fernandes et al., 2001; Minns and Steven, 1977; Prockop and Kivirikko, 1995). This type II collagen fibrillar matrix provides cartilage tissue with important tensile properties. Notably, *Col2a1* also encodes α3(XI) protein chains that are identical to α1(II) chains except that the former are more glycosylated than the latter (Burgeson and Hollister, 1979; Eyre, 1987; Furuto and Miller, 1983).

Alternative splicing of *Col2a1* precursor mRNA (pre-mRNA) is evident during skeletal development with the early inclusion and subsequent exclusion of exon 2 (Ryan and Sandell, 1990). Specifically, chondroprogenitor cells were shown to synthesize exon 2-containing *Col2a1* mRNA transcripts (IIA) while differentiated chondrocytes generate isoforms devoid of exon 2 (IIB) (Lui et al., 1995; McAlinden et al., 2004; Ng et al., 1993; Oganesian et al., 1997; Sandell et al., 1991; Sandell et al., 1994). Exon 2 encodes a 69 amino acid conserved von Willebrand type C-like cysteine-rich domain in the $NH_2$-propeptide of type IIA procollagen. We identified an additional *Col2a1* transcript (IID) that is expressed during chondrogenic differentiation of rabbit and human mesenchymal stem cells (MSCs) and is identical to the IIA isoform except for an additional codon at the 3' end of exon 2 that does not alter the remaining protein coding sequence (McAlinden et al., 2008) (Fig. 1A). The biological significance of the switch from IIA/IID to IIB has not yet been fully elucidated. While we have previously reported on potential mechanisms that regulate exon 2 alternative splicing (McAlinden et al., 2005; McAlinden et al., 2007), it is clear from work presented in this paper that other processes are also involved.

Our group also previously identified another *Col2a1* mRNA isoform (IIC) in pellet cultures of rabbit and human MSC undergoing chondrogenic differentiation by Southern blotting and cDNA sequencing; this isoform is generated by utilization of an alternative 5' splice site within exon 2. Notably, expression of the IIC isoform was observed at an earlier stage of chondrogenic differentiation than the expression of the IIA, IID and IIB splice forms (McAlinden et al., 2008) (Figs. 1A and 1B). The resulting IIC truncated transcript contains the first 34 nucleotides of exon 2 which shifts the reading frame to generate premature termination codons in exon 6. IIC mRNA is therefore a candidate for the nonsense-mediated decay (NMD) process (Brogna and Wen, 2009). Furthermore, no truncated protein was ever

detected by Western blotting using a specific antibody against a putative unique IIC peptide epitope that would arise from a shift in the reading frame (McAlinden et al., 2008). These data suggested that production of the untranslated IIC isoform may represent a transitional mechanism in the production of the subsequent translated *Col2a1* isoforms. Indeed, when part of the IIC 5' alternative splice site was deleted in a human *COL2A1* mini-gene construct, differential mRNA splicing patterns were detected in mouse, human and rat cell lines whereby the ratio of exon 2(+) : exon 2(−) transcripts was increased (McAlinden et al., 2008). To investigate if a similar response to IIC ablation would occur *in vivo*, and to determine if the absence of the IIC isoform would affect cartilage development, we devised a strategy to generate a knock-in transgenic mouse model to disrupt the IIC alternative 5' splice site by introduction of silent point mutations that would not alter the protein coding sequence of exon 2. This study describes successful generation of viable knock-in homozygous (ki/ki) and heterozygous (ki/+) mutant IIC mice (*Col2a1-mIIC*) and their subsequent characterization. Although no overt skeletal or gross morphological phenotype was detected, chondrocytes from ki/ki and ki/+ mice were shown to generate higher ratios of exon 2 (+) : exon 2 (−) transcripts compared to wild type cells. We also show that the exon 2 (+) alpha chains in IIC knock-in mouse cartilage may be incorporated into type XI collagen as well as type II collagen molecules. Although utilization of the IIC 5' splice site produces only low steady-state amounts of IIC mRNA isoforms, this IIC splicing event is clearly involved in a mechanism to regulate the proportions of IIA, IID and IIB procollagen isoforms during cartilage development and maintenance.

## 2. Results

### 2.1. Mutation of the IIC 5' splice site in a COL2A1 mini-gene alters the ratio of mRNA isoforms containing or devoid of exon 2

A human *COL2A1* mini-gene was used in this study that has been previously shown by our group to be a reliable model system to study regulation of exon 2 alternative splicing (McAlinden et al., 2005; McAlinden et al., 2008; McAlinden et al., 2007). Fig. 1B shows the three nucleotide mutation that was created to inhibit the IIC splice site without affecting the protein coding sequence. Fig. 2A shows the position of the 5' and 3' splice sites involved in exon 2 alternative splicing. Each 5' and 3' splice site was scored (Fig. 2B) using MaxEntScan (http://genes.mit.edu/burgelab/maxent/Xmaxentscan_scoreseq.html), a computational tool for analysis of splice site strength based upon dependencies among adjacent and nonadjacent nucleotide positions (Yeo and Burge, 2004). The strength scores of the 5' splice sites were determined using sequences at [-3 to +6] of the 5' splice site, with the GT consensus at positions [+1,+2]. The strength of the 3' splice sites was calculated using sequences at positions [-20 to +3] of the 3' splice site with the AG consensus at [-2,-1] (Table 1). Fig. 2C shows that changing the nucleotides at positions [-2, +1 and +4] of the IIC 5' splice site lowers the splice site score from 6.0 to −5.7, suggesting that spliceosome formation at this region will not occur and IIC splicing will be inhibited.

Splicing of this IIC mutant mini-gene (mIIC) in non-chondrocyte (HEK-293) and chondrocyte (TC28, RCS) cell lines showed a relative increase in the intensity of the major band representing exon 2-containing isoforms (Fig. 1B). Quantitative analysis of all *Col2a1*

isoforms *in vivo* from studies characterizing the *Col2a1-mIIC* transgenic mice has been carried out, and shows a similar change as will be described in this paper. A decrease in the intensity of the band corresponding to isoforms devoid of exon 2 (IIB) was observed in the mIIC mini-gene splice products, compared to splice products of the wild type (WT) mini-gene. The minor, slower-migrating band present in the HEK-293, TC28 and less abundantly in RCS lanes of Fig. 1B likely represents PCR-generated heteroduplexes of different splice form transcripts as has been shown previously in other systems (Claus et al., 2010; McAlinden et al., 2008). In summary, the data presented here shows an alteration in the ratio of *COL2A1* isoforms resulting from IIC splice site mutation in the mIIC *COL2A1* mini-gene. We also generated mIIC minigenes containing an upstream *Hae III* site which was included in the targeting vector for genotyping purposes (Fig. 3A). Introduction of this mutation did not alter splicing of the mIIC mini-gene by cell lines (not shown). These findings motivated us to proceed to generate the transgenic mice with the same three nucleotide mutation at the IIC splice site.

### 2.2. Generation of heterozygous and homozygous Col2a1-mIIC knock-in mice

A targeting vector was generated containing the same silent mutations that were introduced into the *COL2A1* mini-gene (Fig. 3A). The presence of these point mutations in addition to an upstream mutation to create a *Hae III* restriction endonuclease cleavage site for genotyping purposes was confirmed in positive ES clones by PCR with primers Col2a1-F7 and Col2a1-R7 (Table 2, also designated as primers c + d in Fig. 3A), followed by sequencing and *Hae III* restriction digest of the PCR products (not shown). Homologous recombination in three of these ES clones (numbers 142, 174, and 186) was then investigated by Southern blot analysis using probes A, B and internal (INT) (Fig. 3A). Fig. 3B confirms integration of the *Col2a1-mIIC* targeting vector into the correct location within the murine *Col2a1* gene by the presence of expected fragment sizes following *Hind III* digestion of genomic DNA (IIC knock-in mutant DNA fragment size = 9.8kb as detected with Probe A or 4.2 kb as detected with Probes B or INT). Probe INT also confirmed single integration of the knock-in vector. Each of the three positive ES cell clones displayed a normal karyotype (not shown). Injection of two independent positive ES clones (#142 and #174) into C57BL/6J blastocysts followed by implantation into pseudopregnant females resulted in chimeric pups. F1 offspring were generated by crossing male chimeric mice (>95% chimerism) with C57BL/6J female mice (Jackson Laboratory). Germline transmission of the mutant allele was confirmed by PCR analysis with primers Col2a1-loxP-Rev and Z1021 (primers f and o, Fig. 3A; Table 2). Heterozygous mice were bred to EIIa −Cre mice to delete the loxP flanked neomycin selection cassette (Jackson Laboratory Strain Name: B6.FVB-Tg(EIIa-cre)C5379Lmgd/J; Stock Number: 003724). Removal of the neomycin cassette was confirmed by PCR with primers Col2a1-loxP-For and Col2a1-loxP-Rev (Primers e and f, Fig 3A; Table 2) and the genotype of mice from each litter was always confirmed by PCR with primers Col2a1-loxP-For, Col2a1-loxP-Rev and Z1021 (Primers e, f and o; Fig 3A, Table 2). Resulting heterozygous and homozygous mutant mice were viable, obtained with predicted Mendelian frequency and displayed no overt phenotype with respect to overall size and histological (Safranin-O) examination of developing cartilage tissue sections (E16.5 – P56) (results not shown).

### 2.3 Altered Col2a1 mRNA isoform expression in chondrocytes from heterozygous and homozygous Col2a1-mIIC knock-in cartilage tissue

A TaqMan®-based alternative transcript qPCR (AT-qPCR) assay was utilized to accurately quantify levels of the different *Col2a1* mRNA isoforms (IIA, IIB, IIC, IID) *in vivo*. This technology was recently published by our group (McAlinden et al., 2012) and is based upon the utilization of a chemically-synthesized multiple amplicon standard (MAS) plasmid. This MAS plasmid contains amplicons for six custom-designed TaqMan® assays to specifically amplify the IIA, IIB, IIC and IID splice forms as well as the exon 52–53 junction of *Col2a1* (to measure the quantity of total *Col2a1* mRNA) and 18S rRNA as an internal standard.

Embryonic hindlimb buds (E12.5) and an age range of embryonic and post-natal epiphyseal cartilage tissue (E16.5 – P56) was harvested from WT, heterozygous knock-in (ki/+) and homozygous knock-in (ki/ki) *Col2a1-IIC* mice and RNA was extracted for AT-qPCR. Fig. 4 and Table 3 show levels of each *Col2a1* mRNA isoform expressed as a percentage of the total copy number of IIA, IIB, IIC and IID in chondrocytes from WT, ki/+ and ki/ki cartilage at each time point. In WT chondrocytes, IIA is the major isoform produced at E12.5 (∼95%) while IIB mRNA was barely detectable. The IID mRNA isoform (similar to IIA mRNA except for an additional 3 nucleotides at the 3’ end of exon 2; Fig. 1A) represented ∼3% of the four isoforms analyzed. At E16.5, levels of IID mRNA only reached ∼1% in WT chondrocytes and levels were barely detectable at all time points thereafter. The IIC splice form made up only ∼1% of the four isoforms at E12.5 and ∼0.3% at E16.5; at all post-natal time points analyzed, IIC levels were barely detectable or undetectable in WT chondrocytes. By E16.5, the splicing switch from IIA/IID to IIB had occurred in WT cells with IIB mRNA representing ∼72% of the four isoforms analyzed. From P0 onwards, over 90% of mRNA transcripts generated in WT chondrocytes was IIB with higher proportions of IIB present in P14 and P28 chondrocytes. Interestingly, in P56 WT chondrocytes, although IIB is the predominant splice form, the ratio of IIA to IIB transcripts increased compared to that found in P14 and P28 chondrocytes. This ratio was similar to that detected at earlier post-natal time points (P0 and P7).

Homozygous knock-in mutation (ki/ki) of the IIC 5’ splice site resulted in increased ratios of IIA to IIB mRNA isoforms in chondrocytes from all time points analyzed when compared to WT cells (Fig. 4 and Table 3). These differences were particularly more apparent from E16.5 onwards when the IIA to IIB splicing switch had occurred in WT cells. Concomitant with the increase in the percentage of IIA mRNA generated in mutant IIC ki/ki cells was an increase in levels of the IID mRNA isoform when compared to WT cells. As expected, no IIC mRNA was detected in ki/ki chondrocytes at all time points, consistent with ablation of the IIC splice site. As expected, heterozygous mutation of the IIC 5’ splice site resulted in higher ratios of IIA/IID : IIB mRNAs in ki/+ chondrocytes compared to WT cells at each time point and lower ratios compared to homozygous ki/ki cells. Interestingly, of all the post-natal time points analyzed, the highest IIA/IID : IIB ratios in ki/+ and ki/ki chondrocytes were found in chondrocytes of cartilage from 8 week old (P56) mice; these ratios were similar to that produced in ki/+ and ki/ki cells at E16.5.

### 2.4 Mutation of the alternative IIC splice site results in increased expression of IIA procollagen protein isoforms in cartilage ECM of Col2a1-mIIC mice

Immunofluorescence was carried out on paraffin sections of mouse hindlimbs using a specific “anti-IIA” polyclonal antibody (Ab) recognizing the exon 2-encoded cysteine-rich domain in the amino ($NH_2$) propeptide of type II procollagen (Oganesian et al., 1997). In addition to recognizing the exon 2-encoded cysteine-rich (CR) domain of type IIA procollagen, this Ab also recognizes the CR domain present in the “IIA” isoform of type XI procollagen (McAlinden et al., 2013). It is not known if this Ab can also recognize the IID procollagen isoform, but it seems likely since IID differs from IIA procollagen by only one amino acid. In any case, the IID mRNA isoform is expressed at very low levels *in vivo* as shown from the AT-qPCR data (Fig. 4; Table 3). Dual immunofluorescence was also carried out using the anti-IIA Ab and an Ab that recognizes the triple helical domain (THD) of type II procollagen (Cremer and Kang, 1988). Note that this THD Ab recognizes all potential isoforms of type II procollagen (i.e. following processing of type II procollagen to remove the $NH_2$ and COOH propeptides, the THD is the same regardless of whether IIA or IIB procollagen is processed). Figs. 5A–C shows no apparent differences in IIA staining patterns in cartilaginous regions of E12.5 developing limb buds; this is expected given that exon 2-containing IIA isoforms are predominant in cells from all genotypes at this early stage of development (Fig. 4).

Although no histological differences were observed by Safranin-O staining between WT and IIC mutant E16.5 – P56 limb sections (results not shown), differences were noted in the localization of IIA protein, reflecting the increase in IIA : IIB mRNA ratios found at the mRNA level (Fig. 4). At E16.5 and P0, abundant IIA staining was seen at the most proximal end of WT developing tibiae where higher levels of chondroprogenitor cells are present (Fig. 5D,G). However, a “lacy” localization pattern was observed below in the proliferative zone and barely detectable levels were seen in the hypertrophic zone; both of these zones contain chondrocytes further along the differentiation pathway that synthesize predominantly IIB procollagen. The lacy IIA expression pattern in these regions indicates interterritorial matrix localization of remnant protein (most likely the processed IIA $NH_2$-propeptide derived from type IIA procollagen, synthesized at earlier time points of development). Figs. 5E, F, H and I show increased IIA staining patterns in ki/+ and ki/ki tibiae compared to WT. Here, expression can be seen throughout the entire tibiae indicating that differentiated chondrocytes in the proliferative and hypertrophic zones are expressing more IIA-containing procollagen that is being secreted into the ECM. Note that at P0, the size of the WT tissue (Fig. 5G) appears smaller than both ki/+ and ki/ki (Fig. 5H, I) due to the plane of sectioning, and does not reflect a gross morphological difference.

Fig. 6 shows, by dual immunofluorescence, that type II collagen is abundantly expressed in WT P7 cartilage (Fig. 6A; red staining) and that the majority of IIA expression (green staining) remaining is concentrated in the superficial zone of the articular cartilage. However, ki/+ and ki/ki tissue shows abundant IIA expression throughout cartilage of the developing tibia that colocalizes with the triple helical domain of type II collagen (Fig. 6B, C). At this time point, differences can be seen between ki/+ and ki/ki tissue. In ki/+ tissue (Fig. 6B), a loss of IIA staining is noticeable at the most proximal region of the developing

tibia. At P14 when secondary ossification center (SOC) formation is well underway, there is an apparent reduction of IIA staining in the ECM of ki/+ and ki/ki tissue that will become mature articular cartilage (Fig. 6E, F). However, there is still abundant IIA staining in the highly cellular growth plate cartilage region below the SOC in these tissues. P28 images (Fig. 6G, H, I) are of the peripheral region of developing epiphyseal cartilage of the tibiae showing articular cartilage, SOC and the underlying growth plate cartilage. The only area of positive IIA staining in WT tissue was again found at the superficial zone of articular cartilage (Fig. 6G). This superficial zone staining of IIA protein was also found in ki/+ and ki/ki tissue in addition to positive staining in the pericellular domain surrounding a number of chondrocytes located throughout the entire depth of the articular cartilage (Fig. 6H, I). Loss of IIA staining can be seen in the ECM of the upper proliferative zone of growth plate cartilage, but expression is still persistent in the pericellular region of growth plate cartilage cells in the lower proliferative, pre-hypertrophic and hypertrophic regions (Fig. 6H, I).

By 8 weeks of post-natal development (P56), IIA expression persisted in ki/+ and ki/ki articular cartilage at both the superficial zone and in the pericellular domain of deeper zone chondrocytes (Fig. 7B, C) whereas only at the outermost superficial zone region in WT articular cartilage (Fig. 7A). The difference in thickness of the articular cartilage in ki/ki mice (Fig. 7C) compared to WT and ki/+ tissue (Figs. 7A, B) is due only to the plane of sectioning. WT and ki/+ stained tissue sections were obtained from the anterior region of the joint whereas the ki/ki stained section was obtained from a region near the middle of the joint. Persistence of IIA staining was also found in the growth plate of region of ki/+ and ki/ki tissue, especially in the pericellular region of the extracellular matrix (Fig. 7E and F). No IIA staining was observed in the growth plate of P56 WT mice (Fig. 7D).

### 2.5. Persistent expression of the Col2a1 IIA domain in post-natal growth plate cartilage is due, in part, to type XI collagen

The pericellular staining observed with the anti-IIA Ab is reminiscent of type XI collagen staining patterns in cartilage, at least in epiphyseal cartilage tissue (Petit et al., 1993). We therefore investigated whether or not the pericellular staining patterns observed with the anti-IIA Ab in post-natal articular and growth plate cartilage tissue (Figs. 7B, C, E, F) is due to an isoform of the α3(XI) chain of type XI collagen containing the exon 2-encoded CR domain in the retained $NH_2$-propeptide. Since co-immunostaining of the anti-IIA Ab and the anti α1(XI) Ab was not possible, the staining pattern of a tissue section co-stained with the anti-IIA Ab and the type II collagen triple helical domain (THD) Ab was compared to an adjacent tissue section costained with an anti α1(XI) Ab against the thrombospondin domain of the α1(XI) chain (gift from Drs. David Eyre and Russell Fernandes) and the type II collagen THD Ab. Fig. 8 shows that the IIA staining pattern persisting in P56 ki/+ articular cartilage tissue (Fig. 8A) may not due to the presence of type XI collagen since α1(XI) staining in an adjacent P56 ki/+ was below background detection limits (Fig. 8B). Lack of α1(XI) staining in P56 WT articular cartilage tissue was also noted (not shown). However, α1(XI) staining was observed in the pericellular regions of P56 ki/+ growth plate cartilage (Fig. 8D), as was also shown in WT growth plate cartilage (Fig. 8F). This α1(XI) staining pattern in P56 ki/+ growth plate (Fig. 8D) coincides with IIA localization patterns in the adjacent tissue section (Fig. 8C). Similar results were found in P56 ki/ki tissue (results not

shown). Some regions of co-localization (yellow) can be observed in Fig. 8C, but there are also regions showing only IIA but not α3(XI) staining (green) staining. It is possible that the immuno-detected IIA $NH_2$-propeptide is part of the type XI collagen molecule or is perhaps retained in the ECM as a free, cleaved propeptide derived from type IIA procollagen. The same type XI collagen staining patterns were observed in P56 cartilage tissue using an Ab against the variable domain of the α1(XI) chain (gift from Dr. David Birk) (results not shown). Our evidence suggests that anti-IIA Ab staining is detecting the α1(II) chain, and not the α3(XI) chain in articular cartilage at P56. However, it remains possible that the anti-IIA-positive regions in the growth plate of IIC knock-in mice may be due in part to the presence of the exon 2-containing isoform of the α3(XI) chain of type XI collagen.

## 3. Discussion

The present study provides new information on the complexities of *Col2a1* pre-mRNA alternative splicing mechanisms and how these processes control procollagen protein isoform expression patterns during pre- and post-natal development. Our previous studies have identified an additional alternative 5' splice site within *Col2a1* exon 2 that leads to production of a truncated mRNA isoform (IIC) containing the first 34 nucleotides of exon 2 and premature termination codons in exon 6 (McAlinden et al., 2008). A regulatory role for IIC was suggested by our finding that deletion of a 10 nucleotide region of exon 2 overlapping the IIC 5' splice site resulted in an increase in the IIA : IIB ratio expressed by a *COL2A1* mini-gene (McAlinden et al., 2008). In the present study, we found similar alterations in the level of IIA and IIB mRNA when silent point mutations were introduced into the *COL2A1* mini-gene to disrupt the IIC 5' splice site (Fig. 1B). These mutations significantly reduced the strength of the IIC splice site from 6.0 to a value (−5.7), in the range of the weaker IIA (−10.4) and IID (−1.2) 5' splice sites (Fig. 2). These results suggest a possible functional role for the IIC splicing event to regulate exon 2 alternative splicing and control levels of the translatable IIA, IID and IIB transcripts. Mutation of the IIC splice site and alteration of the ratio of transcripts with or without exon 2 may, in turn, impact the development and/or quality of the cartilage extracellular matrix (ECM). Therefore, we were motivated to generate a global knock-in mouse model (*Col2a1-mIIC*) to introduce silent point mutations into the *Col2a1* gene to inhibit the IIC splicing event *in vivo*.

This paper describes successful generation of heterozygous (ki/+) and homozygous (ki/ki) *Col2a1-mIIC* knock-in mice. A splice site targeting approach was used to generate *Col2a1-mIIC* mice, similar to what we reported for production of transgenic *Col2a1*$^{+ex2}$ knock-in mice engineered to express only the IIA isoform of *Col2a1* (Lewis et al., 2012). The fact that no overt skeletal or gross morphological phenotype was observed in *Col2a1-mIIC* mice suggests that the IIC *Col2a1* splicing event is not critical for overall development of cartilage or other non-chondrogenic tissues where *Col2a1* is expressed early in development. However, closer analysis revealed that mutation of this IIC alternative 5' splice site is important in regulating the production of IIA, IID and IIB mRNA isoforms. Using an alternative transcript qPCR method developed and published recently by our group (McAlinden et al., 2012), we were able to quantify levels of IIA, IIB, IIC and IID mRNA in chondrocytes from an age range of cartilage tissue in WT and transgenic knock-in mice (Fig. 4, Table 3). The proportion of IIC mRNA was greatest in WT mice at the earliest time point

(E12.5). Although IIC mRNA could be detected in WT and ki/+ chondrocytes, no IIC transcript was ever detected in ki/ki chondrocytes, as expected. As such, the IIC ki/ki mice provide a “negative control” for the IIC AT-qPCR assay. Levels of IID mRNA were very low, especially in post-natal tissue where IIB mRNA is the major isoform produced. Levels of IID are higher in ki/ki tissue and increase in direct proportion to IIA mRNA production in these cells. The function of the IID splice form remains unknown, and may be distinct from that of the IIA splice form, due to the presence of an additional codon in IID. The relative amounts of IID and IIA in mouse embryonic and postnatal cartilage, chondrogenic human MSC pellet cultures (McAlinden et al., 2008), and during chondrogenesis of ATDC-5 cells (McAlinden et al., 2012) are quite variable. This suggests that these two splicing events do not always occur with the same frequency, merely due to the proximity of the IIA and the IID splice sites.

*Col2a1-mIIC* mice can be regarded as a “mild version” of *Col2a1*$^{+ex2}$ mice that we engineered to exclusively express the IIA isoform of *Col2a1* (Lewis et al., 2012). Similar to *Col2a1*$^{+ex2}$ mice, no overt skeletal phenotype was observed in *Col2a1-mIIC* mice; chondrocyte differentiation, endochondral ossification and formation of secondary ossification center (SOC) occurred as normal in the developing limbs. We showed from our analysis of *Col2a1*$^{+ex2}$ mice that IIA procollagen could be processed (i.e. removal of the $NH_2$ and COOH domains) by differentiated chondrocytes similar to IIB procollagen (Lewis et al., 2012). Therefore, we expect that the increased levels of IIA, and perhaps IID procollagen, produced in *Col2a1-mIIC* mice will be processed to mature type II tropocollagen that will form a covalently cross-linked fibrillar matrix. Evidence for IIA procollagen processing can be seen from immunofluorescent staining patterns of IIA protein in post-natal ki/+ and ki/ki cartilage tissue (P14, P28; Fig. 6). The disappearance of IIA (green) staining from articular cartilage and regions of growth plate cartilage is due to cleavage of the IIA $NH_2$-propeptide from IIA procollagen and subsequent removal from the ECM. The mechanism by which the $NH_2$-propeptide is cleared from the matrix is not known.

Further examination, however, shows persistent staining of IIA protein in the pericellular region of P28 and P56 ki/+ and ki/ki articular and growth plate cartilage (Fig. 6 and Fig. 7). We hypothesize that persistent expression could be due to the presence of type XI collagen, which is known to localize to pericellular regions of epiphyseal cartilage where thinner collagen fibrils are located (Keene et al., 1995; Petit et al., 1993). Type XI collagen is a minor component of cartilage that plays a role in regulating type II collagen fibrillogenesis and fibril diameter (Blaschke et al., 2000). Importantly, *Col2a1* encodes both the α1(II) chain of type II procollagen and the α3(XI) chain of type XI procollagen (Burgeson and Hollister, 1979; Eyre, 1987; Furuto and Miller, 1983). Processing of type XI procollagen is quite complex: the α1(XI) $NH_2$-propeptide is initially retained and later processed after synthesis, the α2(XI) $NH_2$-propeptide is rapidly removed after synthesis while the α3(XI) chain is retained and not processed (Morris and Bachinger, 1987; Thom and Morris, 1991; Wu and Eyre, 1995). The study by Wu and Eyre showed the presence of the IIB $NH_2$-propeptide retained on the α3(XI) chain of type XI collagen in bovine cartilage (Wu and Eyre, 1995). Whether or not IIA isoforms of type XI collagen could exist was only revealed

recently. Specifically, immunoprecipitation analysis of type XI collagen purified from post-natal cartilage of *Col2a1*$^{+ex2}$ mice showed the presence of IIA-containing type XI collagen heterotrimers (McAlinden et al., 2013). Therefore, we found it plausible that the persistent post-natal IIA expression detected in the present study may be due to IIA isoforms of type XI collagen where the exon 2-encoded IIA domain is retained on the $NH_2$-propeptide of the α3(XI) chain. Dual immunostaining of adjacent tissue sections with either the anti-IIA Ab or the anti-α1(XI) Ab showed similar expression patterns in the pericellular region of P56 epiphyseal growth plate cartilage (Fig. 8C and 8D). This shows that persistent expression of IIA protein in post-natal growth plate cartilage is due, in part, to the IIA isoform of type XI collagen. However, we cannot rule out the possibility that some of the positive IIA staining may be due to processed IIA $NH_2$ propeptide derived from type IIA procollagen that exists free in the matrix and has not been removed from the ECM.

The observation that positive anti-α1(XI) domain staining can be detected in maturing epiphyseal growth plate cartilage (Fig. 8D, F) and not in maturing articular cartilage (Fig, 8B) may be due to differences in the molecular architecture of the collagen matrix in both locations. In growth plate cartilage there is an abundance of pericellular matrix relative to inter-territorial and territorial matrix. This pericellular matrix may likely consist of thinner, newly synthesized fibrils still rich in accessible uncleaved IIA $NH_2$-propeptides of type II and XI procollagen. In mature articular cartilage, the lack of α1(XI) staining may be due to more efficient processing of the α1(XI) $NH_2$ propeptide by articular chondrocytes. Alternatively, the epitope may be present, but masked within the type II collagen fibrillar network of articular cartilage (Mendler et al., 1989). Therefore, it is not yet possible to determine what percentage of the persistent IIA staining in post-natal *Col2a1-mIIC* articular cartilage tissue (Fig. 8A) is due to the presence of the α3(XI) chain of type XI collagen. The positive IIA pericellular staining in *Col2a1-mIIC* articular cartilage may be due primarily to the relative abundance of newly synthesized type IIA procollagen in the pericellular matrix. At all stages of post-natal articular cartilage development, IIA staining is localized to the surface/superficial zone not only in ki/+ and ki/ki tissue but also in wild type articular cartilage (Figs. 6D, 6G, 7A). It has been reported previously that the surface of bovine articular cartilage contains a progenitor cell population (Dowthwaite et al., 2004). Therefore, it may be that the persistent IIA staining is due to chondroprogenitor cells at the surface of murine articular cartilage that continually synthesize precursor markers including the “embryonic” isoform of type II procollagen.

The findings presented in this study suggest that IIC splicing may be of regulatory significance in production of *Col2a1* splice forms during cartilage ECM maturation. We propose that, in cells at an early stage of differentiation where chromatin structure has enabled the type II collagen gene to be transcriptionally active, the stronger alternative IIC splice site in exon 2 may be used in preference to the “weaker” IIA/IID splice sites (Fig. 9A). Cells transcribing the non-productive IIC isoform may thus be “poised” in a transitional state leading to productive transcription and splicing of IIA, IID, and ultimately IIB collagen mRNA (Margaritis and Holstege, 2008; Price, 2008). The low levels of the IIC isoform may be related to a low level of *Col2a1* transcription, or to the small number of committed chondroprogenitors in the embryonic and postnatal cartilage relative to

differentiated chondrocytes. In support of this hypothesis, we have previously shown that the IIC splice form is abundant prior to the upregulation of *Col2a1* transcription that accompanies the initial appearance of IIA/D mRNA (McAlinden et al., 2008). This can be easily observed in our pellet culture model for chondrogenesis, in which the differentiation of MSCs is more synchronous than is the differentiation of chondroprogenitors in cartilage. As our model depicts (Fig. 9), the IIA/D procollagen isoforms predominate in chondrocytes at E12.5 (Fig. 9B). This may be due to lower initial RNA polymerase II (pol II) transcription and elongation rates, which can favor spliceosome formation at weak splice sites and inclusion of an alternative exon (de la Mata et al., 2003; Kornblihtt et al., 2004; McAlinden, 2014). It may also be that less mature chondrocytes express higher levels of the necessary accessory splicing factor proteins required to "strengthen" the weak IIA/D 5' splice sites. In fact, we have identified TIA-1 as a nuclear accessory protein that enhances exon 2 splicing (inclusion) (McAlinden et al., 2007); this may be one such factor more highly expressed in chondrocytes early in differentiation. As chondrocytes further differentiate, the rate of *Col2a1* transcription and splicing is significantly increased to support rapid synthesis of the collagen ECM. IIB procollagen formation is favored in this scenario, since spliceosome complexes may not be able to form in enough time at the weak IIA/D splice sites when there are higher rates of transcription and splicing (Fig. 9C). This hypothesis is supported by our finding in this study that mutation of the IIC splice site *in vivo* results in increased levels of IIA and IID procollagen transcripts and decreased levels of IIB procollagen transcripts in P28 differentiated chondrocytes (Fig. 9F) relative to WT (Fig. 9C). This model suggests that *Col2a1* transcription to produce the IIC splice form sets up a "transitional state" in chondrogenesis (a chondroprogenitor cell) that permits the rapid ramping-up of *Col2a1* transcription and splicing to produce the IIA/D splice forms, already under way in E12.5 cartilage. Without the "poising" effect of IIC splicing, progression from IIA/D expression to IIB expression (ECM maturation) may be delayed, as we have observed in the ki/ki mutants. Utilization of the IIA/D 5' splice sites can occur, however, using redundant pathways to provide necessary splicing factors (Fig. 9D and 9E).

It is apparent from our previous studies on the *Col2a1*$^{+ex2}$ mice (engineered only to express the IIA isoform of *Col2a1*) (Lewis et al., 2012) or from our present findings on the *Col2a1-mIIC* mice, that elimination or delay of the IIA/D-to-IIB alternative splicing event does not profoundly disrupt cartilage development as was once believed. Previous studies have suggested a potential role for the exon 2-encoded cysteine rich (CR) domain in regulating TGF-β superfamily growth factor activity during (Larrain et al., 2000; Zhu et al., 1999). The study by Larrain *et al* (Larrain et al., 2000) showed that IIA procollagen over-expression in Xenopus embryos caused a phenotype similar to that of chordin over-expression, thereby suggesting a function in BMP-2/4 inactivation. Therefore, in the *Col2a1*$^{+ex2}$ mice or *Col2a1-mIIC* mice, we expected to observe a chondrodysplasia-like phenotype similar to that reported in the chondrocyte specific *Bmp-2* knock-out mice (Shu et al., 2011). Also, there was no indication of BMP dysregulation in transgenic mice lacking *Col2a1* exon 2 (Leung et al., 2010).

Although gross phenotypic changes were not observed, our studies on *Col2a1*$^{+ex2}$ mice that were engineered to exclusively express the IIA isoforms of type II and type XI collagen

have shown ultrastructural abnormalities in the collagen matrix of knee articular cartilage (unpublished observations) as well as rib cartilage (McAlinden et al., 2013). It is tempting to speculate that mis-expression of "embryonic" isoforms of type II procollagen may affect mechanisms that regulate collagen matrix assembly rather than specific processes related to chondrocyte differentiation and overall cartilage matrix formation. For example, by altering the structure of the $NH_2$ propeptide of type XI collagen (i.e. the addition of the globular exon 2-encoded CR domain in the α3(XI) chain), the function of type XI collagen in regulating fibrillogenesis may be compromised. Also, a recent report showed that a mutation in the $NH_2$-propeptide of type V collagen alters the structure of the $NH_2$-propeptide resulting in abnormal type I collagen fibrils (Symoens et al., 2011). Type V collagen is known to regulate type I collagen fibrillogenesis in a similar fashion to type XI collagen regulating type II collagen fibrillogenesis. Since the ratio of IIA : IIB isoforms has also been altered in *Col2a1-mIIC mice*, it will be interesting in future studies to elucidate the ultrastructure of the collagen matrix in both articular and growth plate cartilage of these mice and to determine whether or not the biomechanical properties of the cartilage has been affected. It will be interesting to look for other markers of immature cartilage in the *Col2a1-mIIC* mutants, to ascertain if aspects of matrix maturation have been affected, which could in turn influence repair. It may be instructive to subject the *Col2a1-mIIC* mice to testing for susceptibility to OA using an established approach to model the disease.

## 4. Experimental Procedures

### 4.1. Construction of wild type and mutant COL2A1 mini-genes

A previously described wild type human *COL2A1* mini-gene (McAlinden et al., 2005) was utilized to generate exon 2 splice site mutant mini-genes. The wild type mini-gene (~5.9kb) consisting of exons 1–3 and full-length introns 1 and 2, was cloned into pcDNA3 vector (Invitrogen) under transcriptional control of the cytomegalovirus promoter. Mutant mini-genes containing the *Col2a1* IIC splice site mutation within intron 2 (*COL2A1-mIIC*) (Fig. 1B) with or without inclusion of an upstream *Hae III* restriction site (Fig. 3A) were generated using the QuikChange™ site-directed mutagenesis kit (Stratagene). PCR mutagenesis was carried out over 18 cycles (95°C, 30s; 55°C, 1min; 68°C, 6min) and resulting PCR products were treated with *Dpn I* (1h, 37°C) to digest parental, methylated DNA. Digested DNA (1μl) was transformed into XL-1 Blue Supercompetent cells (Stratgene) and resulting colonies were screened for presence of the correct mutations.

### 4.2. Transient transfection of COL2A1 mini-genes and analysis of mini-gene spliced mRNA isoforms

The following cell lines were used for transfections: i) HEK-293 human embryonic kidney cells (ATCC), ii) TC28/I2 chondrocytes from human costal cartilage (gift from Dr. Mary Goldring, Hospital for Special Surgery, NY) and iii) RCS (LTC) rat chondrosarcoma cells (Fernandes et al., 1997). Wild type or mIIC mini-gene construct was transfected into each cell line using FuGENE™ 6 reagent (Roche Applied Science) following the manufacturer's protocol. Briefly, 1–3μg of the mini-gene construct was transfected into cells at a ratio of 1:4 DNA:FuGene (μg:μl) for 5h in serum-free medium. Serum-containing medium was then added (final concentration of 10% fetal bovine serum) and the cells were cultured for a

further 48 h. Total RNA was harvested and purified using the RNeasy kit (Qiagen). Reverse-transcribed cDNA was amplified by PCR in the presence of [α-$^{32}$P]dCTP (800Ci/mmol; Perkin Elmer). The primers pcDNA3-COL2A1-Ex1 (5'-CAAGCTTACATGATTCGGC-3') and sp6 were used to amplify cDNA derived only from the exogenously transfected *COL2A1* mini-genes. PCR was carried out for 20x cycles (95°C, 30s; 55°C, 30s; 72°C, 30s). Following addition of 6x loading dye (30% glycerol, 0.025% (w/v) bromophenol blue, 0.025% cyanol blue), an aliquot of resulting PCR products (10μl) was electrophoresed through 6% polyacrylamide gels at 200V. Gels were then dried, exposed to X-ray film and developed the following day.

### 4.3. Generation of a Col2a1-mIIC targeting vector

A mouse 129SvEv BAC (bacterial artificial chromosome, BAC ID# bMQ-131018; Source Bioscience) containing the *Col2a1* genomic locus was used to generate the *Col2a1-mIIC* knock-in targeting vector (Fig. 3A). Mutations were introduced into the BAC using *galK*-based recombineering (Warming et al., 2005), a method that manipulates BACs independently of restriction sites via homologous recombination in bacteria. *Galk* recombineering is a two-step procedure using *galK*-based positive and negative selection. In the initial recombination step, point mutations at the IIC 5' splice site within exon 2 and a silent mutation to create an engineered *Hae III* restriction site (for genotyping purposes) were introduced into the BAC using 50bp *Col2a1* homology arms flanking the *galK* gene. This cassette was generated via PCR using primers Col2a1-IIC-galKrd1-FOR and Col2a1-IIC-galKrd1-REV (Table 4). Clones were obtained via positive selection on minimal media plates containing galactose as the only carbon source. Correctly recombined clones were identified via directional PCR, restriction digest to confirm a lack of BAC rearrangements, and sequencing of PCR products spanning the desired mutations. Positive clones from the first round of recombineering were subjected to a second round of recombineering to remove the *galK* gene, leaving behind only the desired mutations. The recombination cassette was generated by annealing two 100 bp complementary oligos (Col2a1-IIC-galKrd2-FOR2 and Col2a1-IIC-galKrd2-REV2; Table 4) that span the *Col2a1* homology arms used in step 1. Clones were obtained via negative selection on minimal media plates containing glycerol as the only carbon source and 2-deoxy-galactose (DOG) as the selection agent. Clones in which the *galK* cassette has been deleted will grow in the presence of DOG while those retaining the *galK* gene will not. Positive recombinants were identified via directional PCR, restriction digest, and sequencing. A *loxP-neo$^r$-loxP* expression cassette was inserted within a non-conserved region of *Col2a1* intron 2 (approximately 350 bp downstream of exon 2) via another recombineering method (Lee et al., 2001). The targeting vector was generated from the engineered BAC using gap repair (Lee et al., 2001) into a plasmid containing a diphtheria toxin cassette for negative selection in ES cells. Resulting *Col2a1-mIIC* targeting vector DNA was prepared using a Qiagen maxi-prep protocol, linearized by restriction digest with *AscI* and purified by phenol/chloroform extraction. Linearized targeting vector (40 μg) was then used for electroporation into EDJ22 embryonic stem (ES) cells, derived from 129S6/SvEvTac mice.

### 4.4. Embryonic stem cell electroporation and identification of homologously-recombined positive clones

EDJ22 embryonic stem (ES) cells, derived from 129S6/SvEvTac mice and developed at the Washington University Siteman Cancer Center Murine Embryonic Stem Cell Core (http://escore.im.wustl.edu) were grown on gamma irradiated primary mouse embryonic fibroblast (MEF) feeder layers. Linearized, purified IIC *Col2a1-mIIC* targeting vector DNA (40 μg) was electroporated into EDJ22 cells by standardized protocols of the ES Cell Core. Electroporated cells were plated onto MEFs and cultured in the presence of LIF and 600 μg/ml active G418. Individual ES colonies were selected after 6–7 days of G418 selection and grown for subsequent freezing and genomic DNA preparation. Genomic DNA was prepared from over 200 ES cell colonies. Cell pellets were digested overnight at 52°C with proteinase K followed by phenol/chloroform extraction and isopropanol precipitation. Clones were screened for homologous recombination by PCR using a neomycin specific primer and a primer external to the targeting vector short arm (Primers a + b, Fig. 3; Table 2). Presence of the desired mutations was confirmed in PCR-positive ES clones by PCR with primers Col2a1-F7 and Col2a1-R7 (Primers c + d, Fig. 3; Table 2), followed by sequencing and *Hae III* restriction digest of the PCR products. All ES clones tested had the expected mutations. Three ES clones (numbers 142, 174, and 186) were then confirmed for homologous recombination by *Hind III* digestion of genomic DNA and southern blot analysis using two probes outside the targeting arm sequence and one probe that hybridizes to an internal region of the targeting arm (probes A, B and INT, Fig. 3). Karyotype analysis of positive ES clones was performed by the Cytogenetics Core at Washington University.

### 4.5. Generation of Col2a1-mIIC knock-in mice

Two independent ES clones (142 and 174) were injected into C57BL/6J blastocysts by trained technicians in the Mouse Genetics Core at Washington University (http://mgc.wustl.edu). Mouse embryos isolated at 2.5 days pc were incubated to the blastocyst stage, injected with the targeted ES cells, incubated for several hours and then implanted into pseudopregnant female recipients. Pups were born at 19 days gestation and coat color chimerism was apparent within 7–8 days of birth. Male chimeric mice (>95% chimerism) were bred to C57BL/6J female mice (Jackson Laboratory) to generate heterozygote F1 offspring. Germline transmission of the mutant allele was confirmed by PCR analysis with primers Col2a1-loxP-Rev and Z1021 (primers f and o, Fig. 3; Table 2). Heterozygotes were bred to EIIa-Cre mice for deletion of the loxP flanked neomycin selection cassette (Jackson Laboratory Strain Name: B6.FVB-Tg(EIIa-cre)C5379Lmgd/J; Stock Number: 003724). Presence of Cre was confirmed by PCR with primers Cre-For and Cre-Rev (primers g and h; Table 2) and removal of the neomycin cassette was confirmed by PCR with primers Col2a1-loxP-For and Col2a1-loxP-Rev (Primers e and f, Fig. 3; Table 2). Identification of wild type, heterozygous or homozygous mice from each litter was confirmed by PCR of genomic DNA isolated from mouse tails with primers Col2a1-loxP-For, Col2a1-loxP-Rev and Z1021 (Primers e, f and o; Fig. 3, Table 2).

### 4.6. Col2a1 alternative-transcript qPCR (AT-qPCR)

RNA was extracted from cartilage of developing mouse hindlimbs (E12.5 – P56) from WT, heterozygous and homozygous *Col2a1*-mIIC mice. At E12.5, RNA was extracted from whole developing limb buds. At other time points, epiphyseal cartilage was harvested from the developing tibia and femur of the hindlimbs and pooled. RNA extraction was done using Trizol reagent (Invitrogen) following the manufacturer's instructions and finally dissolved in 30–40 μl of RNAse free water and analyzed with a Nanodrop spectrophotometer. To quantify levels of alternatively spliced *Col2a1* isoforms (IIA, IIB, IIC, IID), a TaqMan®-based alternative transcript quantitative PCR (AT-qPCR) assay system was used. This new methodology, developed by our group, was recently published in *Matrix Biology* and readers should refer to this paper for an in-depth description of the method used in this study (McAlinden et al., 2012).

For each sample, an "absolute" value for 18S rRNA was determined, using dilutions of the *Mus musculus Col2a1* MAS (Multiple Amplicon Standard) plasmid (McAlinden et al., 2012) to produce a standard curve. This plasmid contains an insert with amplicons for 18S rRNA, IIA, IIB, IIC, IID splice forms, and the "constitutive" exon 52–53 junction (used to measure total *Col2a1* mRNA). The absolute value of each splice form was normalized to 18S rRNA. For each individual RNA sample, therefore, this normalization allowed the splice form values to be compared to one another. Since 18S rRNA in each sample was derived from all cell types present, which varied between samples, an inter-sample comparison of "absolute" values was not possible. We therefore expressed splice form values for each sample as the percent of the sum of all *Col2a1* splice forms (total of all normalized splice form values).

### 4.7. Immunohistochemistry to detect type II and type XI procollagen protein expression

Hindlimb buds or hindlimbs were harvested and fixed in 10% neutral buffered formalin. Fixation times varied between 1–3 days depending on the age of the tissue. After fixation, samples were rinsed in sterile water and decalcified whenever necessary (E16.5-P70) for a period of time between 12 hr – 2 wk depending on the bone content of the limbs. Fixed, decalcified limbs were then dehydrated, embedded in paraffin and sectioned. Glass slides containing paraffin sections (5 μm) were baked overnight at 56°C, de-paraffinized in xylene, rehydrated through different grades of ethanol and incubated with 1% hyaluronidase (Sigma) for 30 min at 37°C. Sections were rinsed with 1xPBS and blocked with 10% goat serum for 1 h at room temperature and then incubated overnight at 4°C with a rabbit polyclonal "anti-IIA" antibody (Ab) that recognizes the exon 2-encoded cysteine-rich domain within the $NH_2$- propeptide of type II procollagen (1/400 dilution) (Oganesian et al., 1997) and a rat polyclonal Ab against the triple helical domain (THD) of type II collagen (Cremer and Kang, 1988). Each Ab was diluted 1/400 and 1/100, respectively in 2% goat serum. Sequential tissue sections were also dual immuno-stained with a rabbit polyclonal Ab raised against the thrombospondin domain of the α1(XI) chain (gift from Drs. David Eyre and Russell Fernandes) or the variable domain of α1(XI) (gift from Dr. David Birk) and the rat polyclonal type II collagen THD Ab. Each Ab was diluted 1/1000 (Eyre/Fernandes Ab), 1/200 (Birk Ab) or 1/100 (collagen II THD Ab) in 2% goat serum. Following 1x PBS washes, paraffin sections were incubated with species-specific secondary antibodies (1/250

dilution) that were conjugated to Alexa fluorescent dyes [Invitrogen: goat anti-rabbit Alexa 488; goat anti-rat Alexa 594] for 1 h at room temperature. DAPI mounting medium was applied following three rinses in 1x PBS and stained sections were cover-slipped. A Nikon Eclipse E800 fluorescence microscope was used to view the fluorescent images. The FITC and TRITC band pass filter sets were used to view sections labeled with Alexa 488 and 594 dyes, respectively and the DAPI filter set was used for viewing cell nuclei.

## Acknowledgements

We thank the excellent Core facilities at Washington University involved in generating the transgenic mice. These include the Transgenic Vectors Core, The Embryonic Stem Cell Core and the Mouse Genetics Core. We also thank Dr. David Eyre and Dr. Russell Fernandes (University of Washington) and Dr. David Birk (University of South Florida) for type XI collagen antibodies. Thanks also to Crystal Idleburg for histology services provided through the Washington University Musculoskeletal Research Center Core facility (currently funded by an NIH P30 Core Grant: AR057235). This work has received funding from an NIH R21 grant (RR02597; to AM and TMH).

Grant Sponsor: NIH R21 grant RR025397 (AM and TMH); NIH Musculoskeletal Core Grant (P30 AR057235).

## REFERENCES

Blaschke UK, Eikenberry EF, Hulmes DJ, Galla HJ, Bruckner P. Collagen XI nucleates self-assembly and limits lateral growth of cartilage fibrils. J. Biol. Chem. 2000; 275:10370–10378. [PubMed: 10744725]

Brogna S, Wen J. Nonsense-mediated mRNA decay (NMD) mechanisms. Nat. Struct. Moo. Biol. 2009; 16:107–113.

Burgeson RE, Hollister DW. Collagen heterogeneity in human cartilage: identification of several new collagen chains. Biochem. Biophys. Res. Commun. 1979; 87:1124–1131. [PubMed: 465027]

Canty EG, Kadler KE. Procollagen trafficking, processing and fibrillogenesis. J. Cell Sci. 2005; 118:1341–1353. [PubMed: 15788652]

Claus S, Aubert-Foucher E, Demoor M, Camuzeaux B, Paumier A, Piperno M, Damour O, Duterque-Coquillaud M, Galera P, Mallein-Gerin F. Chronic exposure of bone morphogenetic protein-2 favors chondrogenic expression in human articular chondrocytes amplified in monolayer cultures. J. Cell. Biochem. 2010; 111:1642–1651. [PubMed: 21053273]

Cremer MA, Kang AH. Collagen-induced arthritis in rodents: a review of immunity to type II collagen with emphasis on the importance of molecular conformation and structure. Int. Rev. Immunol. 1988; 4:65–81. [PubMed: 3072386]

de la Mata M, Alonso CR, Kadener S, Fededa JP, Blaustein M, Pelisch F, Cramer P, Bentley D, Kornblihtt AR. A slow RNA polymerase II affects alternative splicing in vivo. Mol. Cell. 2003; 12:525–532. [PubMed: 14536091]

Dowthwaite GP, Bishop JC, Redman SN, Khan IM, Rooney P, Evans DJ, Haughton L, Bayram Z, Boyer S, Thomson B, Wolfe MS, Archer CW. The surface of articular cartilage contains a progenitor cell population. J. Cell Sci. 2004; 117:889–897. [PubMed: 14762107]

Eyre D. Collagen of articular cartilage. Arthritis Res. 2002; 4:30–35. [PubMed: 11879535]

Eyre, DR. Type XI or 1a2a3a collagen. In: Mayne, R.; Burgeson, RE., editors. Structure and function of collagen types. New York: Academic Press; 1987. p. 261-281.

Eyre DR, Weis MA, Wu JJ. Articular cartilage collagen: an irreplaceable framework? Eur. Cell Mat. 2006; 12:57–63.

Fernandes RJ, Hirohata S, Engle JM, Colige A, Cohn DH, Eyre DR, Apte SS. Procollagen II amino propeptide processing by ADAMTS-3. Insights on dermatosparaxis. J. Biol. Chem. 2001; 276:31502–31509. [PubMed: 11408482]

Fernandes RJ, Schmid TM, Harkey MA, Eyre DR. Incomplete processing of type II procollagen by a rat chondrosarcoma cell line. Eur. J. Biochem. 1997; 247:620–624. [PubMed: 9266705]

Furuto DK, Miller EJ. Different levels of glycosylation contribute to the heterogeneity of alpha 1(II) collagen chains derived from a transplantable rat chondrosarcoma. Arch. Biochem. Biophys. 1983; 226:604–611. [PubMed: 6639071]

Keene DR, Oxford JT, Morris NP. Ultrastructural localization of collagen types II, IX, and XI in the growth plate of human rib and fetal bovine epiphyseal cartilage: type XI collagen is restricted to thin fibrils. J. Histochem. Cytochem. 1995; 43:967–979. [PubMed: 7560887]

Kornblihtt AR, de la Mata M, Fededa JP, Munoz MJ, Nogues G. Multiple links between transcription and splicing. RNA. 2004; 10:1489–1498. [PubMed: 15383674]

Larrain J, Bachiller D, Lu B, Agius E, Piccolo S, De Robertis EM. BMP-binding modules in chordin: a model for signalling regulation in the extracellular space. Development. 2000; 127:821–830. [PubMed: 10648240]

Lee EC, Yu D, Martinez de Velasco J, Tessarollo L, Swing DA, Court DL, Jenkins NA, Copeland NG. A highly efficient Escherichia coli-based chromosome engineering system adapted for recombinogenic targeting and subcloning of BAC DNA. Genomics. 2001; 73:56–65. [PubMed: 11352566]

Leung AW, Wong SY, Chan D, Tam PP, Cheah KS. Loss of procollagen IIA from the anterior mesendoderm disrupts the development of mouse embryonic forebrain. Dev. Dyn. 2010; 239:2319–2329. [PubMed: 20730911]

Lewis R, Ravindran S, Wirthlin L, Traeger G, Fernandes RJ, McAlinden A. Disruption of the developmentally-regulated Col2a1 pre-mRNA alternative splicing switch in a transgenic knock-in mouse model. Matrix Biol. 2012; 31:214–226. [PubMed: 22248926]

Lui VC, Ng LJ, Nicholls J, Tam PP, Cheah KS. Tissue-specific and differential expression of alternatively spliced alpha 1(II) collagen mRNAs in early human embryos. Dev. Dyn. 1995; 203:198–211. [PubMed: 7655082]

Margaritis T, Holstege FC. Poised RNA polymerase II gives pause for thought. Cell. 2008; 133:581–584. [PubMed: 18485867]

McAlinden A. Alternative Splicing of Type II Procollagen: IIB or not IIB?. Connect. Tissue Res. 20142014 In Press.

McAlinden A, Havlioglu N, Liang L, Davies SR, Sandell LJ. Alternative splicing of type II procollagen exon 2 is regulated by the combination of a weak 5' splice site and an adjacent intronic stem-loop cis element. J. Biol. Chem. 2005; 280:32700–32711. [PubMed: 16076844]

McAlinden A, Havlioglu N, Sandell LJ. Regulation of protein diversity by alternative pre-mRNA splicing with specific focus on chondrogenesis. Birth Defects Res. C Embryo Today. 2004; 72:51–68. [PubMed: 15054904]

McAlinden A, Johnstone B, Kollar J, Kazmi N, Hering TM. Expression of two novel alternatively spliced COL2A1 isoforms during chondrocyte differentiation. Matrix Biol. 2008; 27:254–266. [PubMed: 18023161]

McAlinden A, Liang L, Mukudai Y, Imamura T, Sandell LJ. Nuclear protein TIA-1 regulates COL2A1 alternative splicing and interacts with precursor mRNA and genomic DNA. J. Biol. Chem. 2007; 282:24444–24454. [PubMed: 17580305]

McAlinden A, Shim KH, Wirthlin L, Ravindran S, Hering TM. Quantification of type II procollagen splice forms using alternative transcript-qPCR (AT-qPCR). Matrix Biol. 2012; 31:412–420. [PubMed: 22974592]

McAlinden A, Traeger G, Hansen U, Weis MA, Ravindran S, Wirthlin L, Eyre DR, Fernandes RJ. Molecular properties and fibril ultrastructure of types II and XI collagens in cartilage of mice expressing exclusively the alpha1(IIA) collagen isoform. Matrix Biol. 2013 [Epub ahead of print].

Mendler M, Eich-Bender SG, Vaughan L, Winterhalter KH, Bruckner P. Cartilage contains mixed fibrils of collagen types II, IX, and XI. J. Cell Biol. 1989; 108:191–197. [PubMed: 2463256]

Minns RJ, Steven FS. The collagen fibril organization in human articular cartilage. J. Anat. 1977; 123:437–457. [PubMed: 870478]

Morris NP, Bachinger HP. Type XI collagen is a heterotrimer with the composition (1 alpha, 2 alpha, 3 alpha) retaining non-triple-helical domains. J. Biol. Chem. 1987; 262:11345–11350. [PubMed: 3112157]

Ng LJ, Tam PP, Cheah KS. Preferential expression of alternatively spliced mRNAs encoding type II procollagen with a cysteine-rich amino-propeptide in differentiating cartilage and nonchondrogenic tissues during early mouse development. Dev. Biol. 1993; 159:403–417. [PubMed: 8405667]

Oganesian A, Zhu Y, Sandell LJ. Type IIA procollagen amino propeptide is localized in human embryonic tissues. J Histochem. Cytochem. 1997; 45:1469–1480. [PubMed: 9358849]

Petit B, Ronziere MC, Hartmann DJ, Herbage D. Ultrastructural organization of type XI collagen in fetal bovine epiphyseal cartilage. Histochemistry. 1993; 100:231–239. [PubMed: 8244774]

Price DH. Poised polymerases: on your mark…get set…go. Mol. Cell. 2008; 30:7–10. [PubMed: 18406322]

Prockop DJ, Kivirikko KI. Collagens: molecular biology, diseases, and potentials for therapy. Annu. Rev. Biochem. 1995; 64:403–434. [PubMed: 7574488]

Ryan MC, Sandell LJ. Differential expression of a cysteine-rich domain in the amino-terminal propeptide of type II (cartilage) procollagen by alternative splicing of mRNA. J. Biol. Chem. 1990; 265:10334–10339. [PubMed: 2355003]

Ryan MC, Sieraski M, Sandell LJ. The human type II procollagen gene: identification of an additional protein-coding domain and location of potential regulatory sequences in the promoter and first intron. Genomics. 1990; 8:41–48. [PubMed: 2081599]

Sandell LJ, Morris N, Robbins JR, Goldring MB. Alternatively spliced type II procollagen mRNAs define distinct populations of cells during vertebral development: differential expression of the amino-propeptide. J. Cell Biol. 1991; 114:1307–1319. [PubMed: 1894696]

Sandell LJ, Nalin AM, Reife RA. Alternative splice form of type II procollagen mRNA (IIA) is predominant in skeletal precursors and non-cartilaginous tissues during early mouse development. Dev. Dyn. 1994; 199:129–140. [PubMed: 8204907]

Shu B, Zhang M, Xie R, Wang M, Jin H, Hou W, Tang D, Harris SE, Mishina Y, O'Keefe RJ, Hilton MJ, Wang Y, Chen D. BMP2, but not BMP4, is crucial for chondrocyte proliferation and maturation during endochondral bone development. J. Cell Sci. 2011; 124:3428–3440. [PubMed: 21984813]

Symoens S, Malfait F, Vlummens P, Hermanns-Le T, Syx D, De Paepe A. A novel splice variant in the N-propeptide of COL5A1 causes an EDS phenotype with severe kyphoscoliosis and eye involvement. PLoS ONE. 2011; 6:e20121. [PubMed: 21611149]

Thom JR, Morris NP. Biosynthesis and proteolytic processing of type XI collagen in embryonic chick sterna. J. Biol. Chem. 1991; 266:7262–7269. [PubMed: 2016327]

Warming S, Costantino N, Court DL, Jenkins NA, Copeland NG. Simple and highly efficient BAC recombineering using galK selection. Nucleic Acids Res. 2005; 33:e36. [PubMed: 15731329]

Wu JJ, Eyre DR. Structural analysis of cross-linking domains in cartilage type XI collagen. Insights on polymeric assembly. J. Biol. Chem. 1995; 270:18865–18870. [PubMed: 7642541]

Yeo G, Burge CB. Maximum entropy modeling of short sequence motifs with applications to RNA splicing signals. J. Comput. Biol. 2004; 11:377–394. [PubMed: 15285897]

Zhu Y, Oganesian A, Keene DR, Sandell LJ. Type IIA procollagen containing the cysteine-rich amino propeptide is deposited in the extracellular matrix of prechondrogenic tissue and binds to TGF-beta1 and BMP-2. J. Cell Biol. 1999; 144:1069–1080. [PubMed: 10085302]

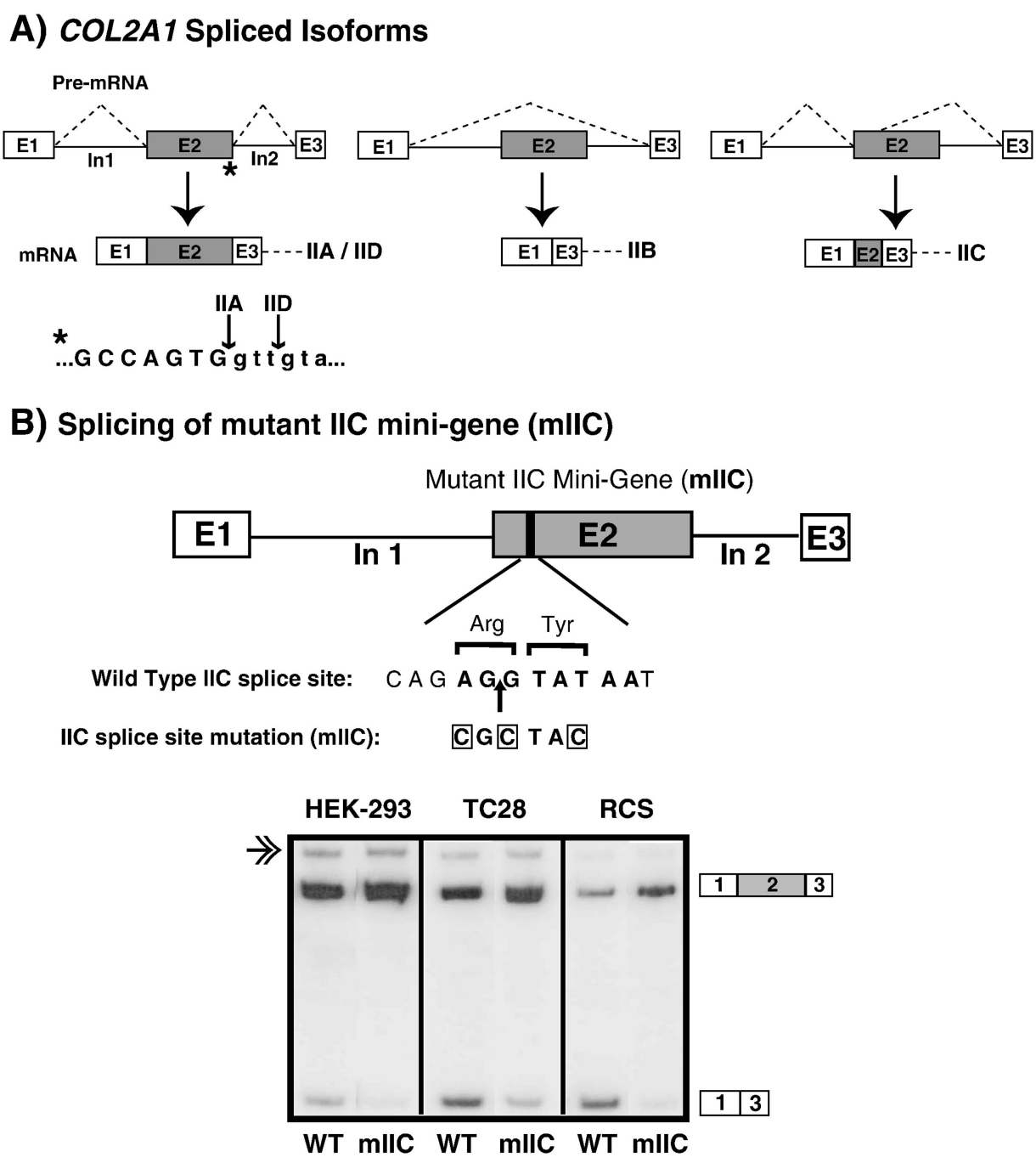


**Fig. 1. *COL2A1* spliced isoforms and the effect of IIC splice site mutation on pre-mRNA alternative splicing**

Panel A shows all potential alternative splicing events involving *COL2A1* exon 2 described to date (McAlinden et al., 2008). Asterisk denotes the exon 2-intron 2 junction containing the IIA and IID 5' splice sites; IIA and IID splicing cleavage sites are also shown. A truncated mRNA product is expected from IIC splicing that contains the first 34 nucleotides of exon 2 (intron and exon sizes not drawn to scale). Panel B shows the composition of the human *COL2A1* mini-gene containing 85bp of exon 1 (from the translation start site) (Ryan

et al., 1990), full-length exons 2 and 3 and full-length intervening introns 1 and 2. The position of the alternative IIC 5' splice site within exon 2 is shown by the vertical black-filled box. The sequence of the IIC 5' splice site is shown in bold font and the arrow denotes the cleavage position of the splice site. The boxed nucleotides show the mutations generated to eliminate the splice site sequence without altering the protein coding sequence (sizes of exons and introns not drawn to scale). The autoradiograph images show PCR products amplified from cDNA of wild type (WT) or mutant mIIC mini-genes in cell lines HEK-293, TC28 and RCS. The position of predicted 386 bp IIA and 179 bp IIB products are indicated. The slower-migrating band indicated by the double arrow may be due to heteroduplex formation of mismatched cDNA strands (Claus et al., 2010; McAlinden et al., 2008).

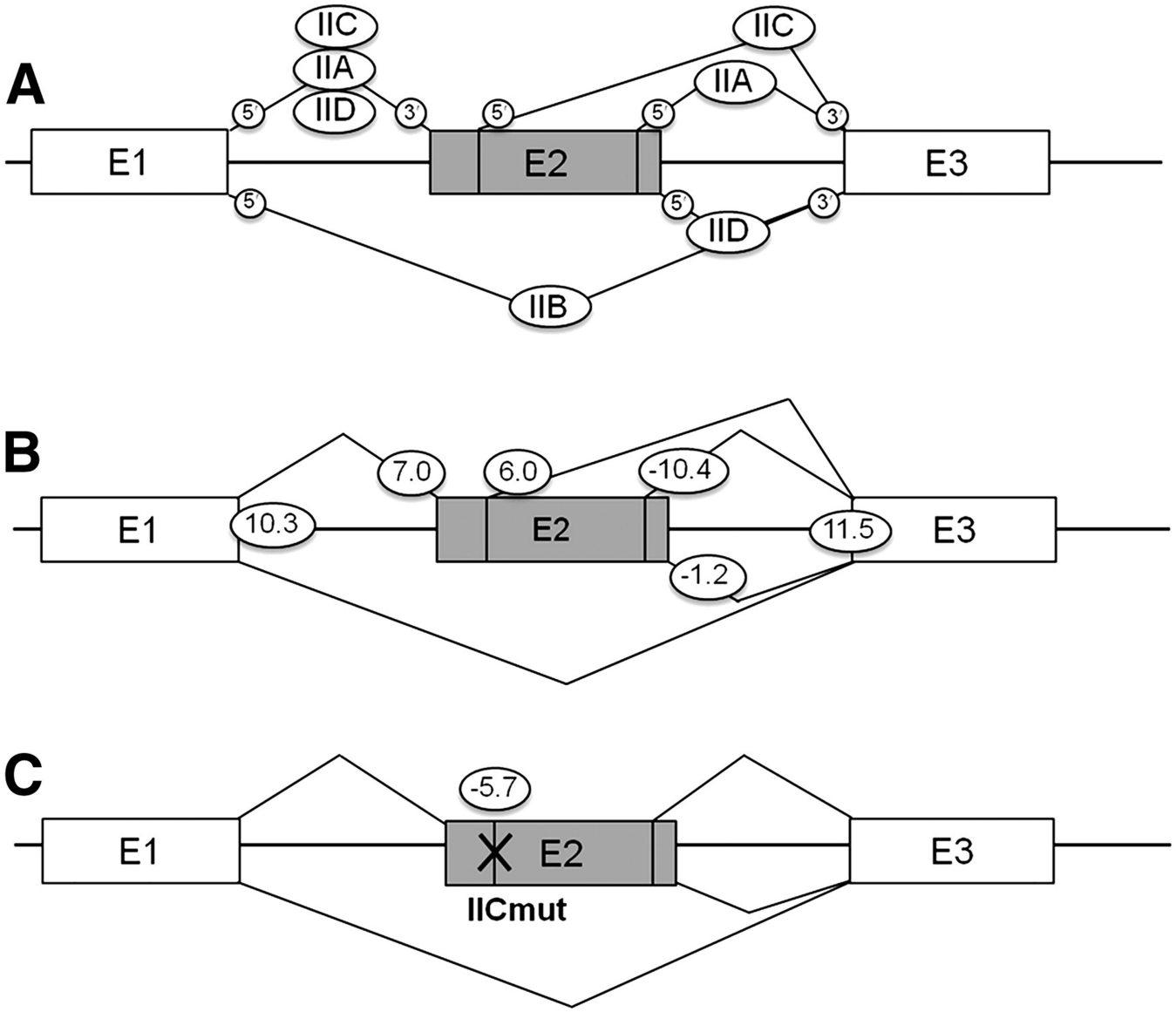


**Fig. 2. Splice site scoring by Maximum Entropy Distribution (MED)**

A) *COL2A1* exon 1 to 3 region, indicating introns which are removed to generate the IIA, IIB, IIC and IID splice forms. B) MED scores are indicated for each potential 5' and 3' splice site. C) The IIC mutant splice site score indicates that there is a low probability of splicing at this site in the mutant (IICmut). MED scores were calculated with MaxEntScan (Yeo and Burge, 2004). See Table 1 for the 5' and 3' splice site sequences analyzed by MaxEntScan.

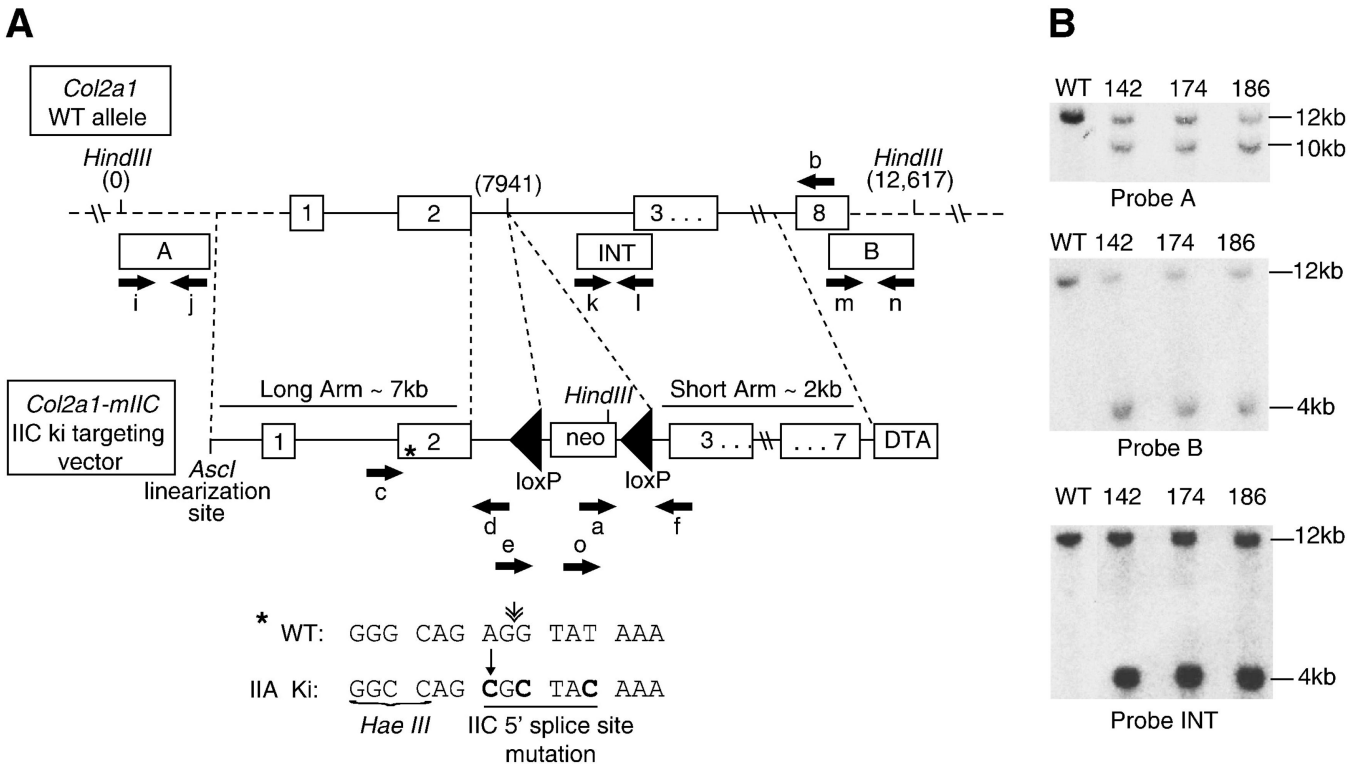


**Fig. 3. IIC splice site knock-in targeting strategy and confirmation of homologous recombination in ES cells**

Panel A shows a region of the wild type (WT) *Col2a1* allele and the targeting vector to generate the *Col2a1-mIIC* knock-in (ki) allele. Location of all primers used to detect homologous recombination and presence of specific point mutations are shown by black arrows (primers a, b, c, d, e, f, and o). Primers i+j, k+l and m+n were used to amplify probes A, INT or B, respectively for use in Southern blotting. Sequences of all primers are shown in Table 2 (including primers g and h which were used to test for the presence of Cre). Asterisk (*) shows the approximate position of the IIC 5' splice site within exon 2 and nucleotide sequence of the splice site is shown below with the double arrow pointing to the cleavage site of the splice site. Underlined sequence shows the three mutated nucleotides (in bold font) that will inhibit splicing at this region. An upstream silent point mutation to create a *Hae III* restriction site, for genotyping purposes, is also shown. Panel B shows radiolabeled Southern blots of *Hind III* digested genomic DNA from homologous recombinant ES clones 142, 174, and 186 and WT control. Southern blot probes A and B confirm homologous recombination within the long and short arms, respectively and probe INT confirms single integration. Expected DNA band sizes are: WT = 12.6 kb with probes A, B, and INT; IIC knock-in mutant = 9.8 kb with probe A and 4.2 kb with probes B and INT.

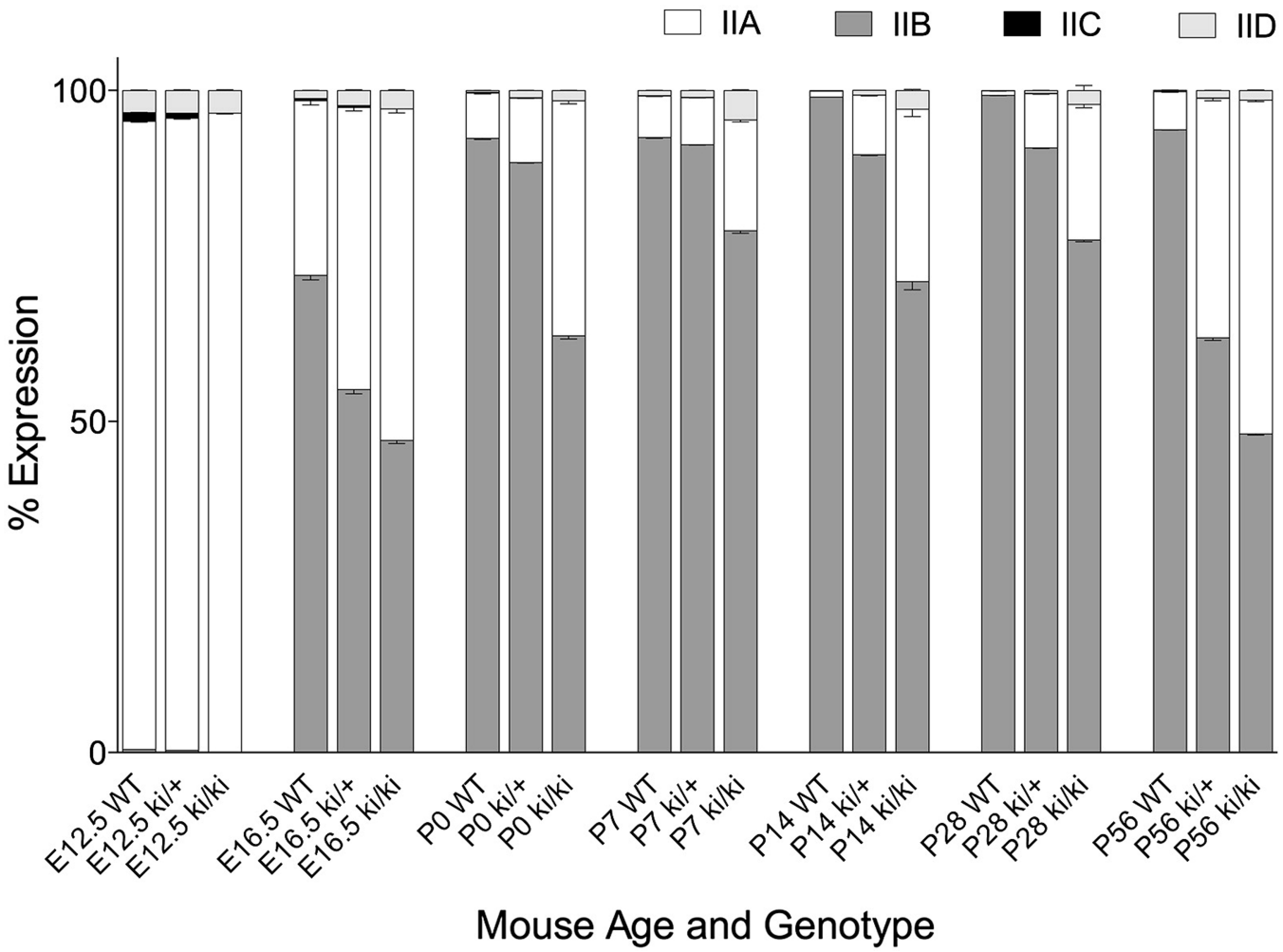


**Fig. 4. AT-qPCR analysis of *Col2a1* alternatively spliced mRNA isoforms (IIA, IIB, IIC, IID) in murine chondrocytes of limb cartilage tissue at different developmental time points**

RNA was extracted from cartilage tissue of wild type (WT), IIC heterozygous knock-in (ki/+) and IIC homozygous knock-in (ki/ki) mice at ages ranging from embryonic (E) day 12.5 to post-natal (P) day 56. Stacked bar graph shows quantified copy numbers of each isoform expressed as a percentage of the total copy number of IIA+IIB+IIC+IID isoforms (see also Table 3).

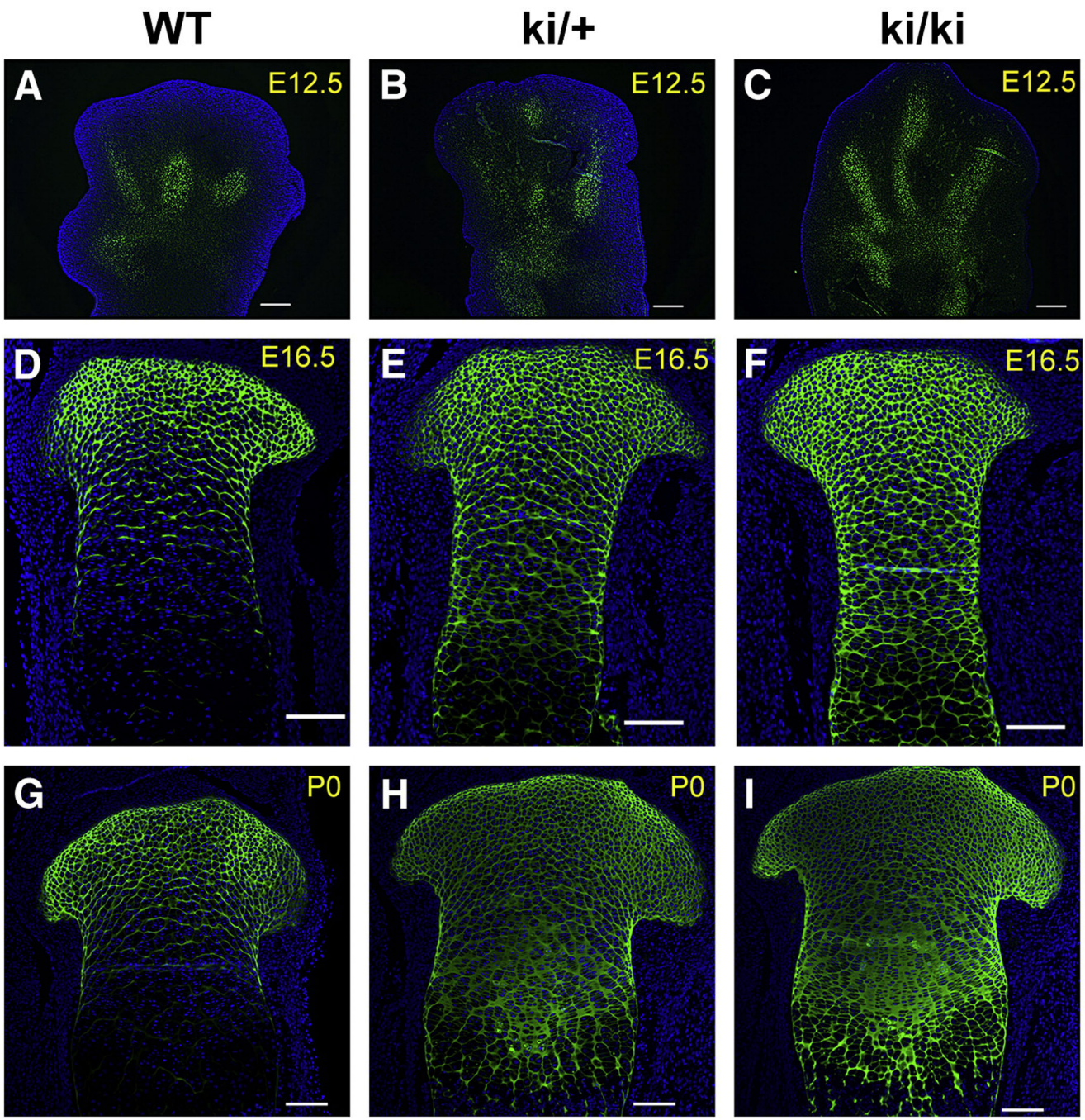


**Fig. 5. Fluorescence immunolocalization of the IIA exon 2-encoded protein domain of *Col2a1***

A polyclonal Ab was used that specifically recognizes the cysteine-rich domain encoded by exon 2 in type IIA procollagen as well as in type XI procollagen. Positive staining (green) was found in cartilage of the developing digits of E12.5 mouse hind limbs as well as in the developing tibiae of E16.5 and P0 mice. Stained cartilage tissue from wild type (WT) mice (Panels A, D, G), IIC heterozygous knock-in (ki/+) mice (Panels B, E, H) and IIC homozygous knock-in mice (Panels C, F, I) is shown. Nuclear (DAPI) staining is shown in blue. Scale bars = 100μm.

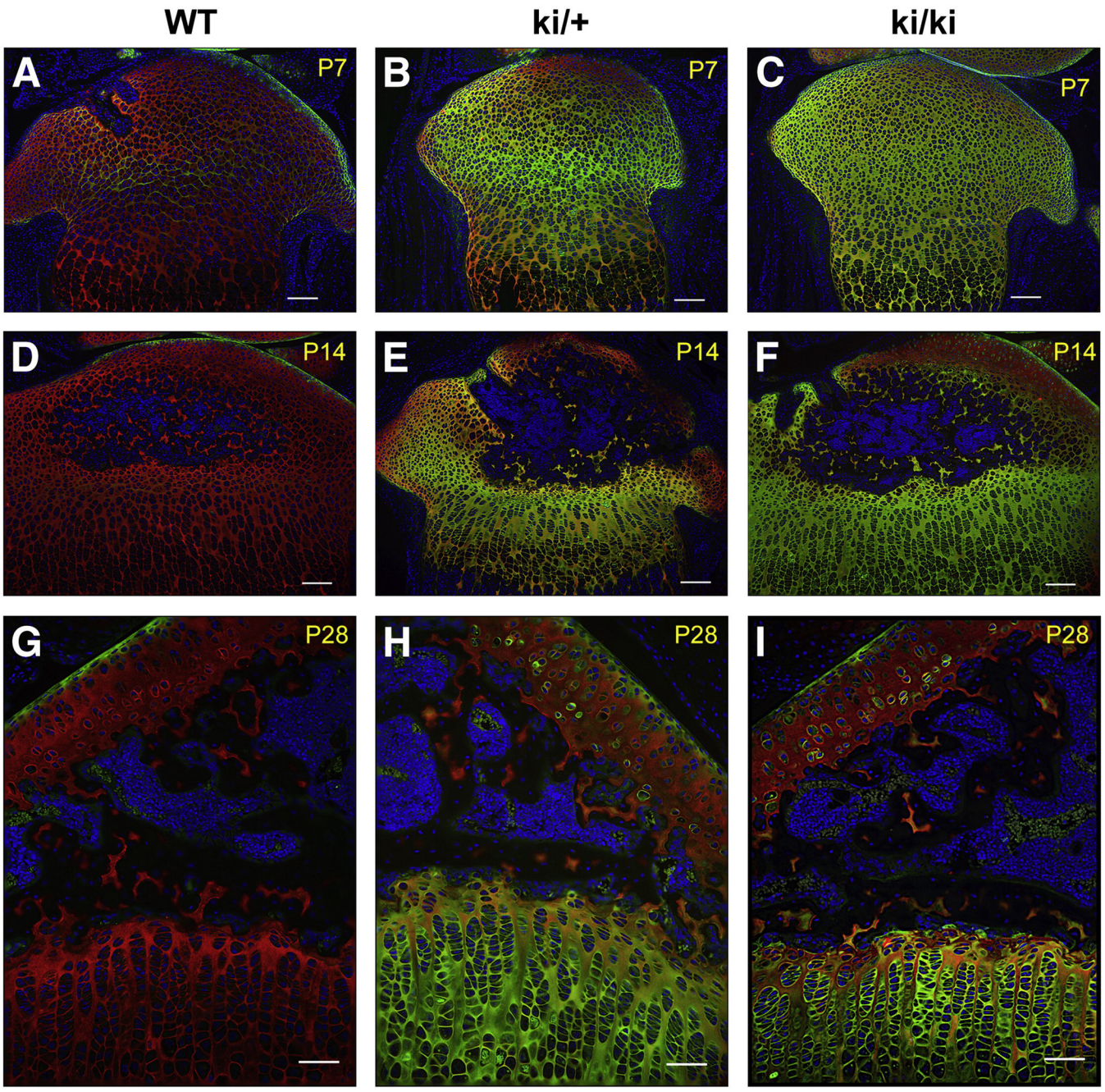


**Fig. 6. Dual fluorescence immunolocalization of the IIA exon 2-encoded domain and the triple helical domain of type II procollagen**

Positive IIA staining (green) and type II collagen triple helical domain staining (red) was found in wild type (WT), heterozygous knock-in (ki/+) and IIC homozygous knock-in (ki/ki) cartilage tissue. Regions of the developing tibiae at post-natal (P) time points P7, P14 and P28 are shown for each genotype: WT (Fig. 6A, D, G); ki/+ (Fig. 6B, E, H) and ki/ki (Fig. 6C, F, I). Panels A–F show the entire developing proximal tibiae and Panels G-I show a region of the proximal tibia near the periphery where articular cartilage subchondral bone

and underlying growth plate cartilage can be observed. Nuclear (DAPI) staining is shown in blue. Scale bars = 100μm (A–F); 50μm (G–I).

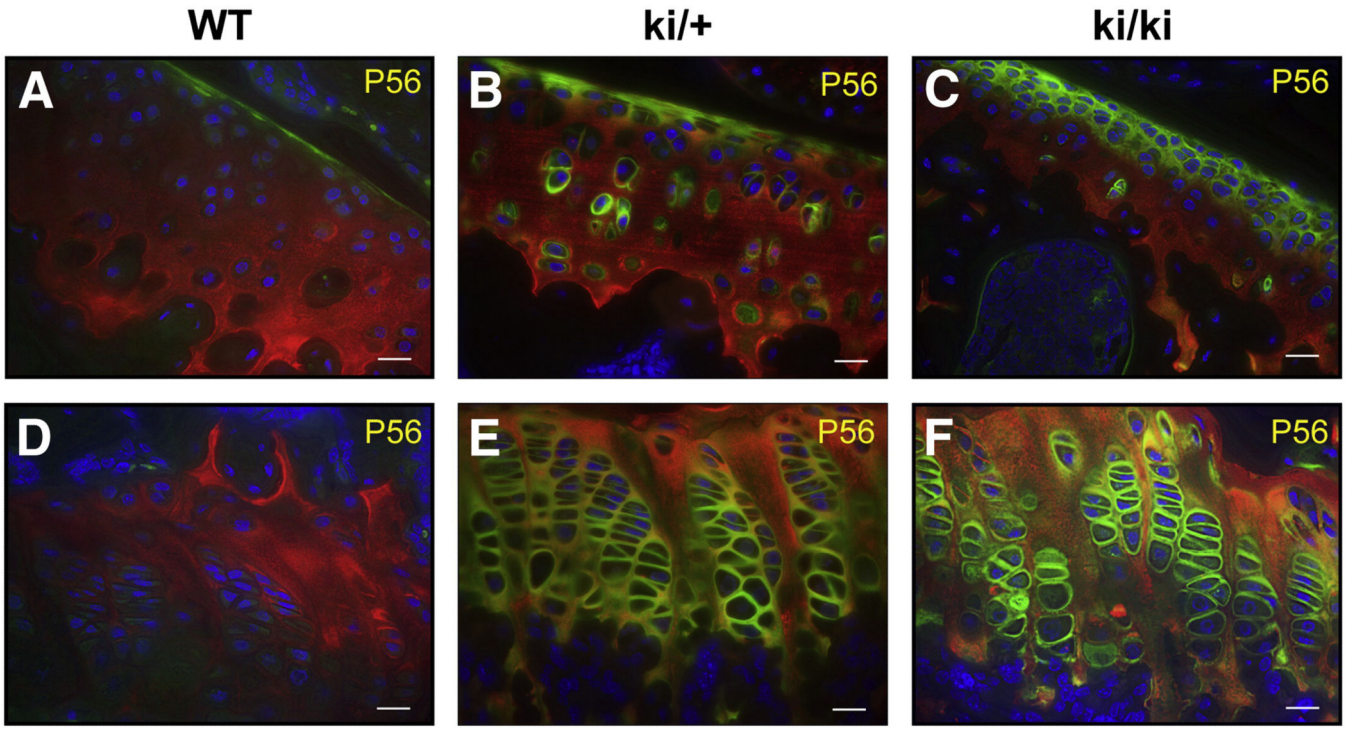


**Fig. 7. Dual fluorescence immunolocalization of the IIA exon 2-encoded domain and the triple-helical domain of type II procollagen in P56 tibial cartilage**

Positive IIA staining (green) and type II collagen triple helical domain staining (red) is shown in wild type (WT), heterozygous knock-in (ki/+) and IIC homozygous knock-in (ki/ki) cartilage. Panels A-C show articular cartilage and Panels D-F show the underlying growth plate cartilage. Note that the difference in articular cartilage thickness shown in Panel C compared to Panels A and B is due to differences in location of the tissue section within the paraffin block. Nuclear (DAPI) staining is shown in blue. Scale bars = 20μm.

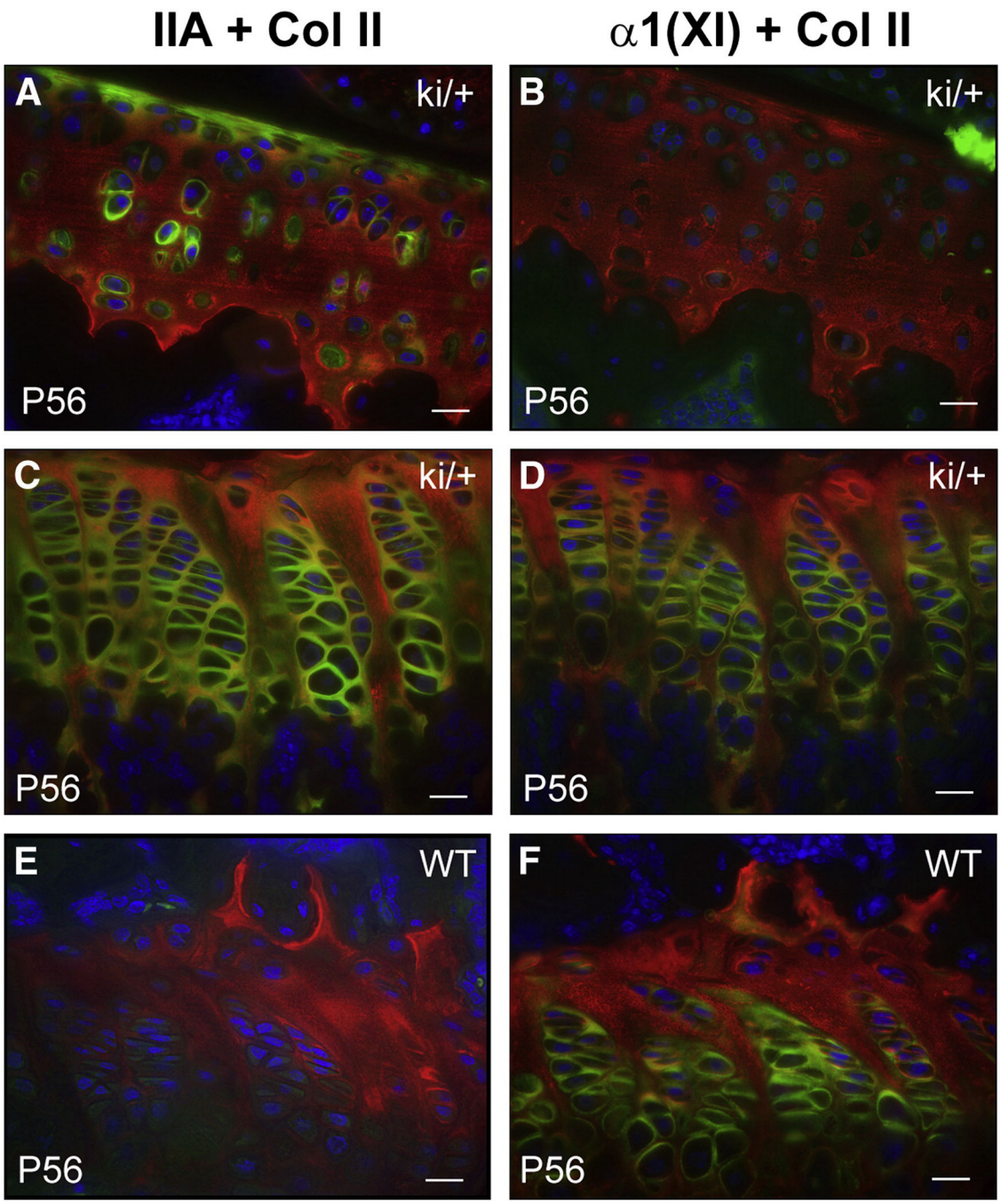


**Fig. 8. Dual immunolocalization of the triple-helical domain of type II procollagen with either the exon 2-encoded IIA domain or the α1(XI) chain of type XI collagen**

Panels A, C and E show dual immunostaining of post-natal (P) day 56 heterozygous knock-in (ki/+) articular cartilage (A) and growth plate cartilage (C) as well as wild type (WT) growth plate cartilage (E) with the anti-IIA Ab (IIA; green) and the Ab recognizing the triple helical domain of type II collagen (Col II; red). Panels B, D and F show dual immunostained images of P56 ki/+ articular cartilage (B), growth plate cartilage (D) and WT growth plate cartilage (F) with the antibodies against the α1(XI) chain of type XI collagen (green) and the

triple helical domain of type II collagen (Col II; red). Nuclear (DAPI) staining is shown in blue. Scale bars = 20μm.

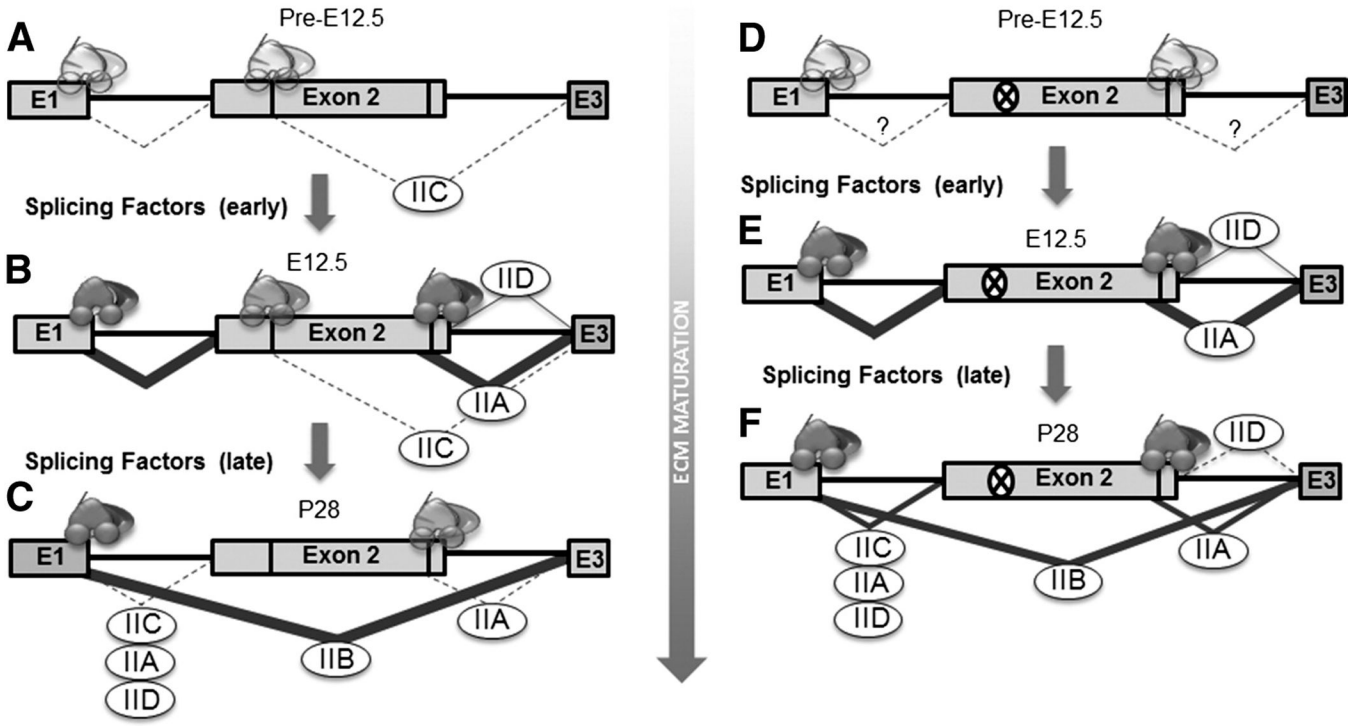


**Fig. 9. Model for regulation of *Col2a1* isoform expression by the IIC splicing event**

During normal chondrogenesis (A–C), the *Col2a1* gene in committed chondroprogenitor cells (pre-E12.5) is transcriptionally active but the rate of transcription of *Col2a1* is low, and the IIC splice form predominates via splicing at the "stronger" IIC splice site (A). At E12.5 (during overt chondrogenesis) via the action of spliceosomes and "early" splicing factors to permit use of the "weak" IIA and IID splice sites, the IIA splice form predominates (B). By P28, the IIB splice form is the most abundant transcript, due to the high strength of the IIB splice sites, specific "late" splicing factors to permit IIB splicing, or lack of splicing factors to permit use of the IIA or IID sites (C). In the IIC knock-in mutant (D–F), the IIC 5' splice site is ablated (D), and no IIC transcript is produced during maintenance of the transcriptionally active state. In the absence of IIC splicing, the production of IIA/D isoforms may commence at embryonic days prior to 12.5 ("?" in Fig. 9D). By E12.5, "early" splicing factors permit predominantly IIA as well as low levels of IID splicing (E). By P28 (F), exon 2 containing isoforms (particularly IIA isoforms) are more abundant in the context of the IIC splice site mutation compared to levels expressed by WT cells at the same time point (C). While IIB splicing has commenced at this stage (F), it is delayed relative to the WT (C). IIC splicing may therefore initially help to maintain a transcriptionally active state of the *Col2a1* gene by production of a nonsense IIC transcript, allowing accelerated differentiation when appropriate accessory splicing factors are present. IIC splicing may also function to compete with the weaker IIA and IID splice sites, permitting more rapid transition to expression of the IIB splice form. Note that the thickness of the lines indicating splicing of introns represents the relative abundance of the spliced transcripts at the indicated time point in development in the presence or absence of the IIC splice site

mutation. Dashed lines indicate low or putative use of splice sites. Spliceosomes are schematically depicted as complexes at splice junctions.

## Table 1

5’ and 3’ splice site sequences to calculate splice site strength

| 5’ splice sites | Position −3 to +6 | 3’ splice sites | Position −20 to +3 |
|---|---|---|---|
| EXON1gt | 5′-TCCgtaagt-3′ | agEXON2 | 5′-cctccccacccttggtgcagAGG-3′ |
| EXON2Cgt | 5′-GAGgtataa-3′ | agEXON3 | 5′-tctatatttttccttgcagGGC-3′ |
| EXON2C$_{mut}$ct | 5′-GCGctacaa-3′ | | |
| EXON2Agt | 5′-GTGgttgta-3′ | | |
| EXON2Dgt | 5′-GTTgtaatt-3′ | | |

Splice site strength was calculated with MaxEntScan (Yeo and Burge, 2004) (http://genes.mit.edu/burgelab/maxent/Xmaxentscan_scoreseq.html). The strength of the 5’ splice sites were scored using sequences at [−3 to +6] of the 5’ splice site, with the GT consensus at positions [+1,+2]. The strength of the 3’ splice sites were scored using sequences at positions [−20 to +3] of the 3’ splice site with the AG consensus at [−2, −1].

## Table 2

Primers to detect homologous recombination, to generate Southern blot probes and to detect the presence of Cre

| Primer Name | Sequence (5’ −3’) | Product Size |
|---|---|---|
| (a) neo-R1 | AGC TGG TTC TTT CCG CCT CAG GAC TCT TCC | a + b: 2.3 kb |
| (b) Col2a1-ES-REV | CCA TAG CTT GCA ATG TAC TTG GCA AGG GCA | |
| (c) Col2a1-F7 | TTC AAA ACT ACT GTG TCA GTT CAG CCT GTC | c + d: 578 bp |
| (d) Col2a1-R7 | GGT CTC TGT AGT GAT TCA GGC TCA CCA GCC | |
| (e) Col2a1-loxP-FOR | AGG CTG GTG AGC CTG AAT CAC TAC AGA GAC | e + f: 321 bp |
| (f) Col2a1-loxP-REV | CTT TGT TAG CAC TGG TTC TAG CTG GGA GTG | |
| (g) Cre-FOR | GCA TTA CCG GTC GAT GCA ACT AGT GAT GAG | g + h: 408 bp |
| (h) Cre-REV | GAG TGA ACG AAC CTG GTC GAA ATC AGT GCG | |
| (i) Col2a1-ES-A-FOR | TAG TTG CAG GAA CTG GAG AGC TG | i + j: 1019 bp |
| (j) Col2a1-ES-A-REV | CTG AGG CTC TGG CCA GAG AGT CTG | |
| (k) Col2a1-ES-INT-FOR | CAG AGG TGA TCG TGG TGA CAA GG | k + l: 617 bp |
| (l) Col2a1-ES-INT-REV | CCA AGG ACA GTG GTC ACT GCT C | |
| (m) Col2a1-ES-B-FOR | GCT AGT CCC TGA TAA CCA GAG AC | m + n: 1006 bp |
| (n) Col2a1-ES-B-REV | CTC ACA GAG ACA CCA GGC TCG C | |
| (o) Z1021 | CGG AGA ACC TGC GTG CAA TCC ATC TTG TTC | f + o: 658bp |

Hybridization locations of these primers are shown in Fig. 3 with the exception of primers g and h.

## Table 3

Quantification of IIA, IIB, IIC and IID mRNA splice forms by AT-qPCR

| *Col2a1mIIC* | IIA (%) | IIB (%) | IIC (%) | IID (%) |
|---|---|---|---|---|
| E12.5 WT | 94.88 | 0.45 | 1.33 | 3.34 |
| E12.5 ki /+ | 95.47 | 0.33 | 0.77 | 3.43 |
| E12.5 ki/ki | 96.57 | 0.01 | 0.00 | 3.42 |
| E16.5 WT | 26.37 | 72.07 | 0.33 | 1.23 |
| E16.5 ki/+ | 42.61 | 54.82 | 0.28 | 2.29 |
| E16.5 ki/ki | 50.04 | 47.15 | 0.00 | 2.81 |
| P0 WT | 6.83 | 92.78 | 0.11 | 0.29 |
| P0 ki/+ | 9.74 | 89.08 | 0.08 | 1.10 |
| P0 ki/ki | 35.51 | 62.93 | 0.00 | 1.56 |
| P7 WT | 6.28 | 92.89 | 0.03 | 0.80 |
| P7 ki/+ | 7.13 | 91.81 | 0.02 | 1.04 |
| P7 ki/ki | 16.77 | 78.80 | 0.00 | 4.43 |
| P14 WT | 0.90 | 99.00 | 0.01 | 0.09 |
| P14 ki/+ | 8.99 | 90.30 | 0.01 | 0.70 |
| P14 ki/ki | 26.06 | 71.12 | 0.00 | 2.82 |
| P28 WT | 0.69 | 99.25 | 0.01 | 0.04 |
| P28 ki/+ | 8.22 | 91.31 | 0.01 | 0.47 |
| P28 ki/ki | 20.48 | 77.42 | 0.00 | 2.11 |
| P56 WT | 5.77 | 94.06 | 0.06 | 0.13 |
| P56 ki/+ | 36.24 | 62.62 | 0.03 | 1.12 |
| P56 ki/ki | 50.40 | 48.14 | 0.00 | 1.46 |

Values are shown as percentage of total *Col2a1* splice forms (See Figure 4).

## Table 4

Primers and oligos used for galK-based recombineering

| Primer/Oligo | Sequence (5'−3') |
|---|---|
| Col2a1-IIC-galKrd-1-FOR | caccccacttggtgcagaggaggctggcagctgtctgcagaatgg*C*cag**C**c ctgttgacaattaatcatcggcat |
| Col2a1-IIC-galKrd-1-REV | cacacagatgcggcaagatgagggcttccatacatccttatctttt**G**ta**G**ct cagcactgtcctgctccttgtg |
| Col2a1-IIC-galKrd-2-FOR2 | caccccacttggtgcagaggaggctggcagctgtctgcagaatgg*C*cag**C**g **C**ta**C**aaagataaggatgtatggaagccctcatcttgccgcatctgtgtg |
| Col2a1-IIC-galKrd-1-REV2 | cacacagatgcggcaagatgagggcttccatacatccttatctttt**G**ta**G**c**G** ctg*G*ccattctgcagacagctgccagcctcctctgcaccaagtggggtg |

GalK-based recombineering was used to introduce mutations into the mouse 129SvEv BAC for production of the *Col2a1-mIIC* targeting vector. Uppercase italics = silent mutation to create the *Hae III site*; Uppercase bold = mutations to inhibit the IIC splice site in exon 2; Underlined lowercase = homology to *galK* sequence.